

Silabutadienes. Internal Rotations and π -Conjugation. A Density Functional Theory Study[†]

Hong-Wei Xi, Miriam Karni,* and Yitzhak Apeloig*

*Schulich Faculty of Chemistry and the Lise Meitner-Minerva Center for Computational Quantum Chemistry, Technion-Israel Institute of Technology, Haifa 32000, Israel**Received: May 1, 2008; Revised Manuscript Received: July 27, 2008*

The potential energy surfaces (PESs) for internal rotation around the central single bond of nine silabutadienes, which include all possible mono-, di-, tri-, and tetrasilabutadienes, are investigated computationally by using DFT with the B3LYP functional and the 6-311+G(d,p) basis set. For 1-silabutadiene (**3**), 2-silabutadiene (**4**), 1,4-disilabutadiene (**5**), 2,3-disilabutadiene (**6**), and 1,3-disilabutadiene (**7**), the *s*-trans rotamer is the most stable. For 1,2-disilabutadiene (**8**), 1,2,3-trisilabutadiene (**9**), and 1,2,4-trisilabutadiene (**10**), all having a trans-bent Si=Si double bond, the most stable conformers are those having an antiperiplanar (ap) structure. For tetrasilabutadiene (**11**), the global minimum is the *gauche* rotamer. The internal rotation barriers (RB) (relative to the global minimum) follow the order (kcal/mol) **5** (10.0) > **3** (7.4) > 1,3-butadiene (**12**, (6.6)) > **10** (4.9) \geq **7** (4.4) \geq **4** (4.0) \approx **8** (3.9) > **9** (2.7) \approx **6** (2.6) > **11** (2.4). The barriers are slightly smaller at CCSD(T)/cc-PVTZ, but the trend remains the same. The size of the rotation barrier is mainly dictated by the length of the central single bond; that is, it is the largest for dienes with the shorter C–C central bond (**5**, **3**, and **12**), and it is smaller for dienes with the longer Si–C and Si–Si central bonds. The strength of π -conjugation in the *s*-trans conformers of silabutadienes was estimated by resonance stabilization energies (RE) calculated by using the Natural Bond Orbital (NBO) and Block Localized Wave function (BLW) methods and bond separation equations. A linear correlation is found between the barrier heights for internal rotation and π -conjugation energies. The calculated RBs are significantly smaller than the corresponding REs, indicating that π -resonance energies are not the only factor that dictate the RB, and therefore, RBs, although suitable for estimating trends in π -conjugation in a series of compounds, **cannot** be used for estimating absolute resonance energies.

Introduction

Double bonds to silicon, such as C=Si and Si=Si, are of great contemporary interest because of their unique fundamental properties and chemistry, as well as their role in polysilane chemistry and material sciences. In the past three decades, the study of compounds containing double bonds to silicon was one of the fastest growing fields of organosilicon chemistry.¹ Yet, this field of chemistry is still in its infancy, and much remains to be learned. For example, little is known on the synthesis and properties of silabutadienes which have two conjugated double bonds. A landmark experimental breakthrough in the field was the synthesis and characterization of the first stable tetrasilabutadiene **1** by Weidenbruch and co-workers in 1997.² X-ray crystallography showed that **1** adopts a *gauche* conformation (C_2 symmetry) with a SiSiSiSi dihedral angle of 51° and Si=Si and Si–Si bond lengths of 2.175 and 2.321 Å, respectively. The authors suggested that conjugation between the two double bonds of **1** exists both in solution and in the solid state.² In 2007, Ichinohe et al. isolated another tetrasilabutadiene derivative **2a**,^{3a} which is also highly twisted (with a SiSiSiSi torsion angle of 72°) and has Si=Si and Si–Si bond lengths of 2.200 and 2.338 Å, respectively, and Kira et al. synthesized and isolated the third known tetrasilabutadiene **2b**,^{3b} which, in contrast to **1** and **2a**, has an anticlinal conformation with a SiSiSiSi dihedral angle of 122.6°. These experimental

achievements are ground breaking, but yet the knowledge of the fundamental properties of silabutadienes, for example, their molecular structure, internal rotation barriers, and the extent of conjugation between the double bonds, is very limited, especially when compared to the wealth of experimental and theoretical data available for 1,3-butadiene.

Most of the current knowledge on silabutadienes comes from theory.^{4–11} There are only few computational studies of potential energy surfaces (PESs) and properties of several mono-, di-, and tetrasilabutadienes, but there are no previous studies of trisilabutadienes. Trinquier and Malrieu⁴ studied the isomerization of 1-silabutadiene (**3**) and of 2-silabutadiene (**4**) to their corresponding silylenes. They found that **4** is more stable than **3** by 5.8 kcal/mol but that the resonance energy (RE) in **4** (calculated by isodesmic equations) is negligible and significantly smaller than that in **3**. Yoshizawa's group investigated the internal rotation around the central C–C single bond in 1,4-disilabutadiene (**5**) by using the DFT B3LYP/6-31G(d,p) level of theory. They found that the most stable conformer is *s*-trans, the *gauche* conformer is less stable, and the *s*-cis conformer is a transition state connecting the two equivalent *gauche* conformations.^{6a} Another study, that investigated electrocyclic ring closure of **5** and **7** to the corresponding silacyclobutenes, found that the *gauche* conformer of 1,3-disilabutadiene **7** is by 5.2 kcal/mol more stable than that of 1,4-disilabutadiene **5** (CASSCF/6-31G(d,p)).⁷ Müller⁸ explored in detail the structure and relative energies of several Si₄H₆ isomers by using the DFT B3LYP/6-311+G(d,p) level of theory and pointed out that the C_i structure of the *s*-trans rotamer of tetrasilabutadiene (**11**) is

[†] Part of the "Sason S. Shaik Festschrift".

* Authors to whom correspondence should be addressed. E-mail: apeloig@tx.technion.ac.il (Y.A.) and chmiri@tx.technion.ac.il (M.K.).

the lowest-energy conformer, by 1.3 kcal/mol lower in energy than the C_{2h} planar structure. He suggested that π -conjugation between the Si=Si bonds dictates the barrier for the internal rotation in **11**, reporting internal barrier heights of 3.8, 2.6, and 10.1 kcal/mol for **11**, **6**, and **5**, respectively. Only few studies investigated the degree of π -conjugation in silabutadienes. Müller⁸ reports that REs in 1,4 disilabutadiene (**5**), 2,3-disilabutadiene (**6**), and tetrasilabutadiene (**11**), calculated by isodesmic equations, follow the order **5** > **11** > **6**. A more recent study by Frenking et al.¹¹ discusses the strength of π -conjugation in s-trans planar conformers of seven silabutadienes (**3**–**8** and **11**) by using energy decomposition analysis (EDA). Their results show that the extent of π -conjugation in monosilabutadienes and disilabutadienes follow the trends **3** > **4** (one silicon atom) and **5** > **7** > **8** > **6** (two silicon atoms). Most of the previous theoretical studies on silabutadienes have been reviewed by Apeloig and Karni.^{1g,i}

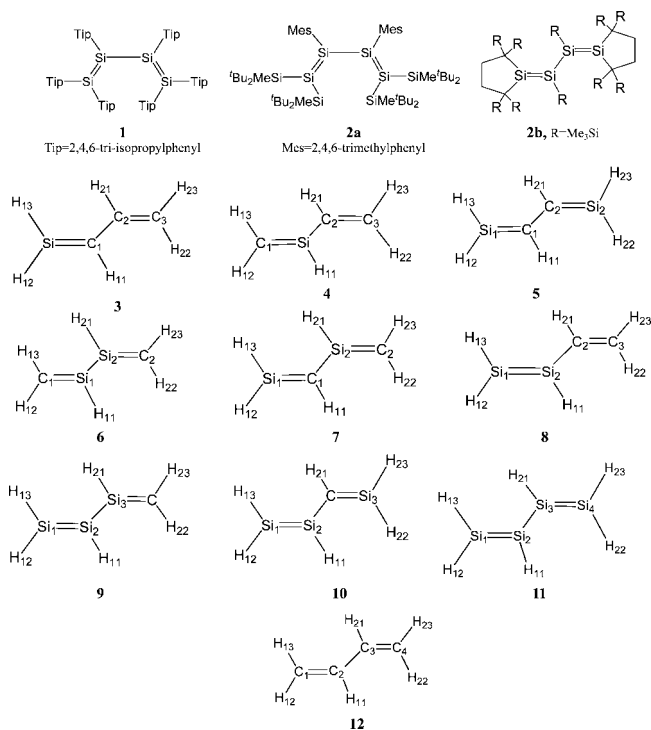
Here, we report a systematic study of the structures and PESs for the internal rotation around the central bonds of all possible isomers of silabutadienes containing one to four silicon atoms, that is, **3**–**11**, and study the relation between the internal rotation barrier heights and the degree of π -conjugation in these dienes. For comparison, the PES for internal rotation in 1,3-butadiene (**12**) was also studied. The strength of π -conjugation in the s-trans conformers of these nine silabutadienes is estimated from conjugative stabilization energies calculated by using the Natural Bond Orbital (NBO) method,^{12,13} the recently developed Block Localized Wave function (BLW) method,¹⁴ and bond-separation energies. The factors that govern the extent of π -conjugation and rotation barrier heights are analyzed, and the implication of π -conjugation on the structures of the s-trans rotamers is discussed.

Methods of Calculation

Most of the calculations were performed with DFT,^{15,16} by using the B3LYP hybrid functional (Becke's three-parameter hybrid functional¹⁷ with the nonlocal correlation of Lee–Yang–Parr^{18a} and VWN3^{18b} local correlation) with the 6-311+G(d,p)¹⁹ basis set.²⁰ Several specific points on the PESs were also optimized with the ab initio MP2 (the second-order Møller–Plesset perturbation theory^{21,22}) and CCSD (coupled cluster theory including single and double excitations²³) levels of theory, using the same basis set. The barriers for internal rotation were also calculated at CCSD(T)^{26b/cc-PVTZ^{26c,d}//B3LYP/6-311+G(d,p)}. The B3LYP results are used as the basis for discussion, unless stated otherwise. All the calculations were carried out by using the Gaussian 03 series of programs.²⁷

The NBO 5.0 program^{12,13} was used to calculate atomic charges and conjugation stabilization energies. REs were also calculated by using the BLW¹⁴ approach, which is implemented in GAMESS.^{28a} For these calculations, we used B3LYP^{28b} with the 6-311G(d,p) basis set. In the BLW method, all electrons and primitive basis functions are divided into several subgroups. In the block localized wave function, each MO is restricted to be expanded in a subgroup of the basis functions. The BLW is subjected to the restriction that MO orbitals within each subgroup are orthogonal, whereas those belonging to different subgroups are nonorthogonal. The energy difference between the Kohn–Sham (KS) wave function, in which the electrons are allowed to delocalize over the whole system, and that of the BLW, in which the π -electrons are confined to specific zones, represents the RE. Two types of resonance energies (REs) are calculated: the vertical RE (VRE), in which the geometry of the hypothetical localized structure is the same as that of the

SCHEME 1



delocalized one, and an adiabatic RE (ARE), in which the geometry of the localized structure is relaxed. The difference between VRE and ARE reflects the compression energy of the σ frame.¹⁴ To calculate VRE and ARE of the subject silabutadienes, the electrons in each diene were divided into three subgroups: two separate subgroups, each containing the π -electrons of a single double bond (π -electrons are localized on the double bond) and the third subgroup containing all the σ -electrons. For each silicon atom, we included in the localized π -electron subgroups, in addition to the valence π -electron, also two 2p core electrons and their respective primitive basis functions having the π -direction. A representative input example is given in the Supporting Information.

The term internal rotation refers to internal rotation around the central M^2 – M^3 single bond in $H_2M^1=M^2H-M^3H=M^4H_2$ ($M^i = C, Si$). The internal rotational angle, θ , is the $M^1M^2M^3M^4$ torsion angle. The PESs for internal rotation ($E(\theta)$ versus θ) were obtained by performing anticlockwise rotations around the central M^2 – M^3 single bond at a set of selected θ values ranging from 180° to -180° with full geometry optimization at each point. Frequency calculations were performed for the stationary points along the PESs in order to confirm them as minima or transition states and to evaluate zero-point energies (ZPEs).

Stereochemical notations of the various rotational conformers are as follows: conformers with $M^1M^2M^3M^4$ dihedral angles of 0 and 180° are called s-cis and s-trans, respectively. Stationary points with $M^1M^2M^3M^4$ torsional angle in the range between $+30$ and $+90^\circ$ and between -30 and -90° are termed gauche, and those which are rotated slightly from s-cis (with torsion angles in the range between 0 and $\pm 30^\circ$) and from s-trans (in the range between ± 180 and $\pm 150^\circ$) are notated synperiplanar (sp) and antiperiplanar (ap), respectively. Conformers with torsion angles in the range between $+90$ and $+150^\circ$ are termed anticlinal (ac).²⁹

The atom numbering in silabutadienes **3**–**12** used in the discussions are shown in Scheme 1.

TABLE 1: Relative Energies (kcal/mol) of Stationary Points along the Internal Rotation Paths of Silabutadienes 3–11 and 1,3-butadiene 12^{a,b}

dienes	s-trans	ap	TS(t-g)	gauche	s-cis	gauche ^c	TS(g-t) or TS(c-t) ^c
CH ₂ =SiHCH=CH ₂ (4)	0.0 (0.0), [0.00] ^d		4.22 (4.02) 3.55 ^e	1.77 (1.67)	1.78 (1.56)	1.77 (1.67)	4.22 (4.02)
SiH ₂ =CHCH=CH ₂ (3)	0.0 (0.0), [1.58] ^d		7.92 (7.42) 6.65 ^e	3.16 (3.07)	3.46 (3.27)	3.16 (3.07)	7.92 (7.42)
SiH ₂ =SiHCH=CH ₂ (8)	0.0 (0.0), [0.00] ^d	-0.49 (-0.37, -0.53) ^f	3.63 (3.52) 2.91 ^e		1.40 (1.29)	0.75 (0.82)	3.24 (3.09)
SiH ₂ =CHSiH=CH ₂ (7)	0.0 (0.0), [6.29] ^d		4.62 (4.37) 3.70 ^e	1.46 (1.33)	1.46 (1.26)	1.46 (1.33)	4.62 (4.37)
CH ₂ =SiHSiH=CH ₂ (6)	0.0 (0.0), [9.42] ^d		2.61 (2.59) 2.12 ^e		1.13 (1.08)		2.61 (2.59)
SiH ₂ =CHCH=SiH ₂ (5)	0.0 (0.0), [12.95] ^d		10.45 (10.01) 8.66 ^e	3.87 (3.80)	4.17 (4.00)	3.87 (3.80)	10.45 (10.01)
SiH ₂ =SiHCH=SiH ₂ (10)	0.0 (0.0), [0.00] ^d	-0.67 (-0.55, -0.80) ^f	4.53 (4.39) 3.28 ^e		1.73 (1.59)	1.03 (1.09)	4.90 (4.67)
SiH ₂ =SiHSiH=CH ₂ (9)	0.0 (0.0), [0.32] ^d	-0.21 (-0.15, -0.27) ^f	2.58 (2.55) 1.81 ^e		1.00 (0.91)	0.64 (0.78)	2.22 (2.17)
SiH ₂ =SiHSiH=SiH ₂ (11)	0.0 (0.0) ^g	-0.78 (-0.51, -1.32) ^f	1.51 (1.84) 0.84 ^e		0.09 (0.40)	-0.84 (-0.51)	2.03 (2.08)
CH ₂ =CHCH=CH ₂ (12)	0.0 (0.0) ^h		7.03 (6.56) 6.13 ^e	3.52 (3.45)	3.97 (3.79)	3.52 (3.45)	7.03 (6.56)

^a At B3LYP/6-311+G(d,p); values in parentheses are the relative energies corrected with ZPEs. ^b The M¹M²M³M⁴ dihedral angles of all stationary points are given in Tables 2 and 3. ^c For $\theta = 0$ to -180° ^d Values in square brackets are the relative energies (including ZPE corrections) of the s-trans conformers in each of the silabutadiene families. The total energies of CH₂=SiHCH=CH₂ (**4**), SiH₂=SiHCH=CH₂ (**8**), and SiH₂=SiHCH=SiH₂ (**10**) are -407.337186, -658.736404, and -910.126595 au, respectively. ^e At CCSD(T)/cc-PVTZ//B3LYP/6-311+G(d,p). ^f At MP2/6-311+G(d,p). ^g In the planar C_{2h} geometry. The total energy (including ZPE correction) of planar C_{2h} **11** is -1161.528432 au. It is by 1.36 kcal/mol less stable than the nonplanar C_i **11**, which is the most stable conformer. ^h Total energy (including ZPE correction) of **12** is -155.950046 au.

Results and Discussion

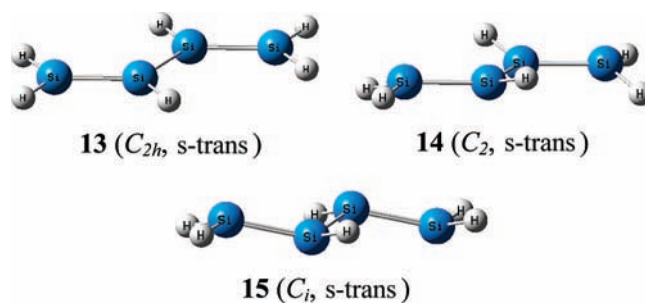
The discussion is divided into two parts: (1) discussion of the PESs for internal rotation and the optimized geometries of the stationary points along the PESs and (2) discussion of the strength of π -conjugation in the s-trans conformers and the correlation between π -conjugation and the barrier height for internal rotation.

I. PESs for Internal Rotation in Silabutadienes. The relative energies of the stationary points on the rotational PESs of silabutadienes **3–11** and of 1,3-butadiene (**12**) are given in Table 1. Their geometries are presented in Table 2 (for **3–7** and **12**) and Table 3 (for **8–11**). The Cartesian coordinates of all structures and a schematic ball-and-stick presentation of the structures are provided in the Supporting Information.

General features. The external double bonds (CH₂=CH-, SiH₂=CH-, and CH₂=SiH-) in silabutadienes **3–7** and in 1,3-butadiene (**12**) remain planar throughout the rotation process. The structures of **3–7** at a specific dihedral angle θ are identical to those of their mirror rotamers (i.e., at $-\theta$). Accordingly, their PESs possess a mirror symmetry; that is, the PES for $\theta = 0$ to 180° is a symmetric mirror image of the PES for $\theta = 0$ to -180° . In contrast, the Si=Si double bonds of 1,2-disilabutadiene (**8**), 1,2,3-trisilabutadiene (**9**), and 1,2,4-trisilabutadiene (**10**) have a trans-bent geometry of C₁ symmetry along the entire rotation path. For 1,4-disilabutadiene (**5**), 2,3-disilabutadiene (**6**), and 1,3-butadiene (**12**), C₂ symmetry is kept throughout the rotation.

For tetrasilabutadiene (**11**), we examined three s-trans structures, planar C_{2h} (**13**), C₂ (**14**), and C_i (**15**). We could not locate the C₂ conformation at B3LYP because it collapsed upon geometry optimization to the planar C_{2h}, but it was located at MP2 and CCSD. However, the C_{2h} and C₂ conformations are both not minima on the PES. The planar C_{2h} structure has at B3LYP two imaginary frequencies (-240.9 and -110.1 cm⁻¹), reflecting a propensity for bending to the trans-bent C₂ or C_i structures, and a small imaginary frequency (-36.1 cm⁻¹) is found at MP2 for the C₂ structure (Table 3). Thus, the most stable s-trans structure, and the only minimum at B3LYP and MP2, has a trans-bent C_i conformation (**15**). However, the energy difference between conformations **13–15** is small: $\Delta E(C_{2h} - C_i) = 1.4$ kcal/mol at both B3LYP (as also reported in ref 8) and CCSD(T)/cc-PVTZ, and $\Delta E(C_2 - C_i) = 2.2$ and

2.6 kcal/mol at MP2 and CCSD, respectively and 1.4 kcal/mol at CCSD(T)/cc-PVTZ.³⁰



a. PESs of Mono- and Disilabutadienes, 3–7. This group of silabutadienes has one or two C=Si bonds, but no Si=Si bond. The PESs for internal rotation of the mono- and disilabutadienes **3–7** and for 1,3-butadiene (**12**) are shown in Figures 1 and 2. As the PESs for $\theta = 180$ to 0° are mirror images of those for $\theta = 0$ to -180° , we will discuss here only one half of the PES. For silabutadienes **3–7**, the s-trans conformer is the global minimum, and the gauche conformer (for **3** and **5**), sp (or gauche, see below) conformers for **4** and **7** and s-cis conformer for **6** are higher energy minima on the rotational PESs (Figures 1 and 2).

The PESs for 1-silabutadiene (**3**), 1,4-disilabutadiene (**5**), and 1,3-butadiene (**12**) have similar general features. Along the PESs ($\theta = 180-0^\circ$), we located two conformers that are minima: s-trans at $\theta = 180^\circ$ and gauche at $\theta = 31.6, 35.2,$ and 32.5° , respectively, which are higher in energy by 3.2, 3.9, and 3.5 kcal/mol, respectively. Two transition states were located, TS(t-g) at $\theta = 101.5, 100.4,$ and 100.5° which connects the s-trans and gauche minima and TS(g-g) that has a s-cis conformation ($\theta = 0^\circ$) and connects the two mirror image gauche minima (Figures 1 and 2, Table 2). TS(t-g) is significantly higher in energy than TS(g-g) (Table 1). Similar PESs for 1,4-disilabutadiene (**5**) and 1,3-butadiene (at B3LYP/6-31G(d,p)) were reported previously by Yoshizawa et al.^{6a}

On the PES of 2,3-disilabutadiene (**6**), we located two planar minima having s-trans and s-cis conformations and a transition

TABLE 2: Calculated Important Geometry Parameters for the s-trans, TS (t-g), Gauche (or sp), And s-cis Stationary Points on the PESs for Internal Rotation of Silabutadienes 3–7 and of 1,3-Butadiene (12)^a

parameter	s-trans	TS(t-g)	gauche or sp	s-cis
CH₂=CHCH=CH₂ (12) (C_{2h})^b				
$\theta(D(C_1C_2C_3C_4))$	180.0	100.5	32.5 (40.1 ^c , 40.5 ^d)	0.0
$r(C_1C_2)^e$	1.338	1.332	1.336 (1.346 ^c , 1.344 ^d)	1.337
$r(C_2C_3)^f$	1.456	1.486	1.469 (1.472 ^c , 1.481 ^d)	1.470
$r(H_{11}H_{21})$	3.109	2.861	2.461 (2.539 ^c , 2.532 ^d)	2.386
$D(H_{11}C_2C_3H_{21})$	180.0	98.1	29.4 (37.1 ^c , 37.3 ^d)	0.0
imaginary frequency ^g	— ^h	−185.7	— ^h	−137.9
SiH₂=CHCH=CH₂ (3) (C_s)^b				
$\theta(D(SiC_1C_2C_3))$	180.0	101.5	31.6 (42.4 ^c)	0.0
$r(SiC_1)^e$	1.728	1.717	1.726 (1.728 ^c)	1.728
$r(C_1C_2)^f$	1.445	1.482	1.456 (1.465 ^c)	1.454
$r(C_2C_3)^e$	1.345	1.334	1.343 (1.350 ^c)	1.344
$r(H_{11}H_{21})$	3.106	2.870	2.433 (2.530 ^c)	2.366
$D(H_{11}C_1C_2H_{21})$	180.0	99.9	25.9 (36.5 ^c)	0.0
imaginary frequency ^g	— ^h	−190.4	— ^h	−105.7
CH₂=SiHCH=CH₂ (4) (C_s)^b				
$\theta(D(C_1SiC_2C_3))$	180.0	98.4	12.5 (32.0 ^c , 31.7 ^d)	0.0
$r(C_1Si)^e$	1.710	1.708	1.711 (1.713 ^c , 1.713 ^d)	1.711
$r(SiC_2)^f$	1.845	1.867	1.854 (1.851 ^c , 1.857 ^d)	1.854
$r(C_2C_3)^e$	1.340	1.337	1.339 (1.350 ^c , 1.348 ^d)	1.339
$r(H_{11}H_{21})$	3.748	3.462	2.959 (3.101 ^c , 3.082 ^d)	2.943
$D(H_{11}SiC_2H_{21})$	180.0	95.8	11.7 (32.30 ^c , 31.6 ^d)	0.0
imaginary frequency ^g	— ^h	−185.7	— ^h	−40.4
SiH₂=CHCH=SiH₂ (5) (C_{2h})^b				
$\theta(D(Si_1C_1C_2Si_2))$	180.0	100.4	35.2 (46.9 ^c , 45.0 ^d)	0.0
$r(Si_1C_1)^e$	1.742	1.722	1.739 (1.735 ^c , 1.734 ^d)	1.740
$r(C_1C_2)^f$	1.428	1.475	1.437 (1.457 ^c , 1.463 ^d)	1.435
$r(H_{11}H_{21})$	3.103	2.877	2.415 (2.536 ^c , 2.493 ^d)	2.338
$D(H_{11}C_1C_2H_{21})$	180.0	99.8	22.0 (35.8 ^c , 32.0 ^d)	0.0
imaginary frequency ^g	— ^h	−211.8	— ^h	−90.8
CH₂=SiHSiH=CH₂ (6) (C_{2h})^b				
$\theta(D(C_1Si_1Si_2C_2))$	180.0	97.6	0.0	0.0
$r(C_1Si_1)^e$	1.718	1.716	1.718	1.718
$r(Si_1Si_2)^f$	2.299	2.321	2.307	2.307
$r(H_{11}H_{21})$	4.491	4.165	3.588	3.588
$D(H_{11}Si_1Si_2H_{21})$	180.0	93.3	0.0	0.0
imaginary frequency ^g	— ^h	−74.2	— ^h	— ^h
SiH₂=CHSiH=CH₂ (7) (C_s)^b				
$\theta(D(C_1Si_1Si_2C_2))$	180.0	99.6	13.3 (37.3 ^c , 36.3 ^d)	0.0
$r(Si_1C_1)^e$	1.719	1.712	1.718 (1.719 ^c , 1.717 ^d)	1.718
$r(C_1Si_2)^f$	1.818	1.842	1.825 (1.827 ^c , 1.832 ^d)	1.824
$r(Si_2C_2)^e$	1.713	1.710	1.713 (1.715 ^c , 1.714 ^d)	1.713
$r(H_{11}H_{21})$	3.721	3.475	2.907 (3.098 ^c , 3.069 ^d)	2.886
$D(H_{11}C_1Si_2H_{21})$	180.0	100.8	12.1 (38.0 ^c , 36.2 ^d)	0.0
imaginary frequency ^g	— ^h	−115.2	— ^h	−28.9

^a At B3LYP/6-311+G(d,p), unless otherwise stated. For atom numbering, see Introduction. For stereochemical notations, see the Methods of Calculation and Figures 1 and 2. Bond distances (r) in Å and dihedral angles (D) in degrees. $r(C-H)$ ranges from 1.083 to 1.091 Å, and $r(Si-H)$ ranges from 1.473 to 1.479 Å. All bond angles are within the range of 121.5–134.0°. ^b Symmetry of the s-trans rotamers. ^c At MP2/6-311+G(d,p); other parameters are close to the values at B3LYP. ^d At CCSD/6-311+G(d,p); the CCSD calculation of **3** did not converge. All other parameters are similar to those calculated at B3LYP. ^e C=C, C=Si, and Si=Si bond lengths in CH₂=CH₂, CH₂=SiH₂, and SiH₂=SiH₂ are 1.329, 1.708, and 2.173 Å, respectively (at B3LYP/6-311+G(d,p)). ^f C-C, C-Si, and Si-Si bond lengths in CH₃-CH₃, CH₃-SiH₃, and SiH₃-SiH₃ are 1.531, 1.885, and 2.354 Å, respectively (at B3LYP/6-311+G(d,p)). ^g In cm⁻¹. ^h Minimum.

state (TS(t-c)) at $\theta = 97.6^\circ$ connecting them (Table 2); no gauche minimum was located (Figure 2). On the PESs of **4** and **7**, we located in addition to the s-trans minimum also sp conformers ($\theta = 12.5$ and 13.3° , respectively) which lie in a very shallow minimum (Figures 1 and 2), being 1.77 and 1.46 kcal/mol, respectively, higher in energy than the s-trans conformer. The s-cis conformers which are not minima are less stable than the s-trans by 1.78 and 1.46 kcal/mol, respectively. We reoptimized the geometries of the stationary points of silabutadienes **4** and **7** by using also B3LYP/6-311++G(3df,3pd), MP2/6-311+G(d,p), and CCSD/6-311+G(d,p) methods. At B3LYP, increasing the basis set to 6-311++G(3df,3pd) has a

negligible effect on the structures or energies of the stationary points. However, for the sp conformer of **7**, we find that θ increases significantly from 13.3° at B3LYP to 37.3 and 36.3° at MP2 and CCSD, respectively (24.3° at CASSCF⁷). These structures are by 0.28 and 0.52 kcal/mol, respectively, lower in energy than those of the s-cis structures. A similar increase in θ to 32.3 and 31.7° is found at MP2 and CCSD, respectively, for the sp rotamer of 2-silabutadiene (**4**). However, the rotational PES is very flat, and rotation of, for example, **4** from $\theta = 32.3^\circ$ to $\theta = 12.5^\circ$ requires only 0.05 kcal/mol (MP2, 0.18 kcal/mol at B3LYP). Thus, we conclude that the PESs of 2-silabutadiene (**4**) and of 1,3 disilabutadiene (**7**) have a shape similar to that

TABLE 3: Calculated Important Geometry Parameters of the s-trans, ap, TS(t-g), Gauche, and TS(g-t) Stationary Points on the PESs for Internal Rotation of Silabutadienes 8–11^a

parameter	s-trans	ap	TS(t-g) ^b	s-cis	gauche	TS(g-t) ^c
SiH₂=SiHCH=CH₂ (8) (C₁)^d						
θ (<i>D</i> (Si ₁ Si ₂ C ₁ C ₂))	180.0	159.4 (154.2) ^e	78.8	0.0	-48.1	-125.5
<i>r</i> (Si ₁ Si ₂)	2.170	2.182	2.173	2.180	2.185	2.177
<i>r</i> (Si ₂ C ₁)	1.850	1.852	1.877	1.859	1.862	1.875
<i>r</i> (C ₁ C ₂)	1.341	1.341	1.336	1.339	1.339	1.337
<i>r</i> (H ₁₁ H ₂₁)	3.734 (3.732) ^e	3.730 (3.732) ^e	3.730	2.945	2.944	3.417
<i>A</i> (Si ₁ Si ₂ C ₁)	122.8	122.3	122.3	125.5	122.9	122.1
<i>A</i> (Si ₂ C ₁ C ₂)	124.2	124.0	125.2	127.1	124.6	123.9
<i>D</i> (H ₁₁ Si ₂ C ₁ H ₂₁)	195.9 (197.9) ^e	186.1 (183.5) ^e	109.8	28.1	-13.0	-91.8
<i>D</i> (H ₁₁ Si ₂ Si ₁ H ₁₂)	-31.3 (33.5) ^e	-38.2 (-38.6) ^e	-35.8	-34.1	-42.8	-37.2
<i>D</i> (H ₁₁ Si ₂ Si ₁ H ₁₃)	186.0 (184.3) ^e	184.9 (182.2) ^e	183.3	188.0	181.5	183.0
$\sum\alpha^f$	349.6	345.9	348.7	346.6	345.1	348.0
imaginary frequency ^g	- <i>h</i>	- <i>h</i>	-121.8	-33.4	- <i>h</i>	-109.4
SiH₂=SiHSiH=CH₂ (9) (C₁)^d						
θ (<i>D</i> (Si ₁ Si ₂ Si ₃ C))	180.0	162.9 (155.9) ^e	78.7	0.0	-45.6	-123.1
<i>r</i> (Si ₁ Si ₂)	2.167	2.174	2.166	2.167	2.175	2.170
<i>r</i> (Si ₂ Si ₃)	2.293	2.295	2.321	2.301	2.304	2.319
<i>r</i> (Si ₃ C)	1.719	1.719	1.717	1.718	1.719	1.717
<i>r</i> (H ₁₁ H ₂₁)	4.460 (4.428) ^e	4.458 (4.435) ^e	4.246	3.614	3.586	4.119
<i>A</i> (Si ₁ Si ₂ Si ₃)	120.5	119.8	119.4	123.2	120.9	119.2
<i>A</i> (Si ₂ Si ₃ C)	123.5	123.5	124.4	125.5	123.2	121.6
<i>D</i> (H ₁₁ Si ₂ Si ₃ H ₂₁)	195.6 (199.7) ^e	188.0 (185.2) ^e	110.6	30.5	-4.4	1.3
<i>D</i> (H ₁₁ Si ₂ Si ₁ H ₁₂)	-25.3 (-29.7) ^e	-31.3 (-33.2) ^e	-28.9	-24.5	-34.5	-30.8
<i>D</i> (H ₁₁ Si ₂ Si ₁ H ₁₃)	181.0 (179.3) ^e	181.2 (178.0) ^e	179.2	182.0	178.2	178.8
$\sum\alpha^f$	355.1	353.0	354.5	355.2	352.5	353.9
imaginary frequency ^g	- <i>h</i>	- <i>h</i>	-74.2	-13.3	- <i>h</i>	-67.5
SiH₂=SiHCH=SiH₂ (10) (C₁)^d						
θ (<i>D</i> (Si ₁ Si ₂ CSi ₃))	180.0	157.5 (150.9) ^e	77.4	0.0	-45.7	-122.3
<i>r</i> (Si ₁ Si ₂)	2.197	2.205	2.180	2.200	2.204	2.176
<i>r</i> (Si ₂ C)	1.820	1.822	1.850	1.828	1.830	1.849
<i>r</i> (CSi ₃)	1.724	1.723	1.713	1.721	1.721	1.714
<i>r</i> (H ₁₁ H ₂₁)	3.700 (3.707) ^e	3.698 (3.704) ^e	4.246	3.522	2.880	2.890
<i>A</i> (Si ₁ Si ₂ C)	124.4	124.3	123.4	127.1	125.2	123.3
<i>A</i> (Si ₂ CSi ₃)	126.5	125.7	127.0	130.6	126.7	126.4
<i>D</i> (H ₁₁ Si ₂ CH ₂₁)	191.4 (191.3) ^e	183.2 (180.0) ^e	110.5	26.7	-9.8	-93.4
<i>D</i> (H ₁₁ Si ₂ Si ₁ H ₁₂)	-39.1 (-38.0) ^e	-43.5 (-43.2) ^e	-37.6	-38.1	-48.1	-34.3
<i>D</i> (H ₁₁ Si ₂ Si ₁ H ₁₃)	191.9 (188.3) ^e	189.8 (185.9) ^e	184.4	193.7	184.8	185.3
$\sum\alpha^f$	338.9	337.0	346.8	338.5	337.4	348.4
imaginary frequency ^g	- <i>h</i>	- <i>h</i>	-119.1	-32.2	- <i>h</i>	-113.7
SiH₂=SiHSiH=SiH₂ (11) (C_{2h})^{d,i}						
θ (<i>D</i> (Si ₁ Si ₂ Si ₃ Si ₄))	180.0	142.8 (131.4) ^j	65.4	0.00	-65.6	-144.8
<i>r</i> (Si ₁ Si ₂)	2.155 (2.158 ⁱ , 2.167 ^k , 2.187 ^l)	2.175	2.171	2.178	2.187	2.161
<i>r</i> (Si ₂ Si ₃)	2.274 (2.282 ⁱ , 2.302 ^k , 2.296 ^l)	2.285	2.321	2.307	2.302	2.310
<i>r</i> (H ₁₁ H ₂₁)	4.478 (4.392 ⁱ , 4.3440 ^k , 4.416 ^l)	4.437 (4.415) ^j	3.863	3.846	3.512	4.176
<i>A</i> (Si ₁ Si ₂ Si ₃)	123.8 (121.2 ⁱ , 121.2 ^k , 119.6 ^l)	122.8	121.6	121.0	120.3	119.9
<i>D</i> (H ₁₁ Si ₂ Si ₃ H ₂₁)	180.0 (-142.2 ⁱ , -132.6 ^k , 180.0 ^l)	189.8 (189.9) ^j	47.0	71.2	-11.0	-92.6
<i>D</i> (H ₁₁ Si ₂ Si ₁ H ₁₂)	0.00 (-23.3 ⁱ , -28.7 ^k , -35.9 ^l)	-30.4 (-33.1) ^j	-31.0	-28.8	-38.7	-22.5
<i>D</i> (H ₁₁ Si ₂ Si ₁ H ₁₃)	180.0 (182.7 ⁱ , 183.0 ^k , 181.3 ^l)	182.8 (180.4) ^j	178.9	184.4	178.6	180.6
$\sum\alpha^f$	360.0 (355.1 ⁱ , 352.3 ^k , 350.0 ^l)	352.0	353.7	352.2	349.9	356.3
imaginary frequency ^g	-204.9, -110.1 (-36.1) ^j	- <i>h</i>	-61.5	-22.8	- <i>h</i>	-108.6

^a At B3LYP/6-311+G(d,p), unless otherwise stated. For atom numbering, see Introduction. For stereochemical notations, see the Methods of Calculation and Figures 1 and 2. Bond distances (*r*) in Å, bond angles (*A*), and dihedral angles (*D*) in degrees. *r*(C–H) bondlengths ranges from 1.084 to 1.090 Å; *r*(Si–H) ranges from 1.471 to 1.491 Å. ^b For $\theta = 180$ to 0° . ^c For $\theta = 0$ to -180° . ^d Symmetry of the s-trans rotamers. ^e At MP2/6-311+G(d,p). Other parameters are similar to those at B3LYP and are not given here. ^f The sum of *A*(H₁₂Si₁Si₂), *A*(H₁₃Si₁Si₂), and *A*(H₁₂Si₁H₁₃) bond angle. ^g In cm⁻¹. ^h Minimum. ⁱ The geometry parameters of the s-trans at B3LYP/6-311+G(d,p) are for the planar C_{2h} symmetry or as indicated otherwise. All other stationary points on the PES are at C₂ symmetry. Details of the geometric parameters of the s-trans rotamer at C_{2h}, C₂, and C_i symmetry at B3LYP, MP2, and CCSD are given in the Supporting Information. ^j At MP2/6-311+G(d,p), C₂ symmetry. ^k At CCSD/6-311+G(d,p), C₂ symmetry. ^l At B3LYP/6-311+G(d,p), C_i symmetry.

of 1-silabutadiene (**3**) and of 1,4-disilabutadiene (**5**), whereas the PES of 2,3-disilabutadiene (**6**) is slightly different. The transition states (TS(t-g)) of **4** and **7** are located at $\theta = 101.5$ and 99.6° , respectively (see Table 2).

The lowering of the relative energies of the s-cis conformers of **4** and **7** and the disappearance of the gauche conformer in **6** are attributed to the relatively long Si–Si and Si–C central single bonds, which decrease the steric hindrance for rotation around these bonds. The smaller steric hindrance in the s-cis conformers of **4**, **6**, and **7** is also indicated by their

significantly longer *r*(H₁₁H₂₁) distances (Table 2). Thus, the PESs of **4** and **7** in the vicinity of the s-cis conformer are flatter than those of **3**, **5**, and **12**, having the shorter C–C bond, and the s-cis conformer of 2,3-disilabutadiene (**6**) changes from a TS to a minimum, whereas no gauche conformer is located.

For silabutadienes **3–7** and for 1,3-butadiene, the rotation barriers for the s-trans \rightarrow gauche processes follow the order (kcal/mol, in brackets at CCSD(T)/cc-PVTZ//B3LYP/6-311+G(d,p)): 10.0 [8.7] (**5**) > 7.4 [6.7] (**3**) > 6.6 [6.1] (**12**) >

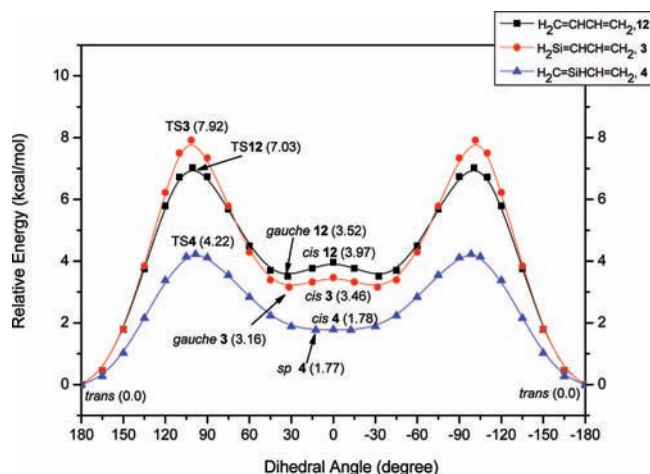


Figure 1. PESs for internal rotation of 1-silabutadiene (**3**), 2-silabutadiene (**4**), and 1,3-butadiene (**12**). The energies (without ZPEs, kcal/mol) are relative to the *s*-trans rotamer.

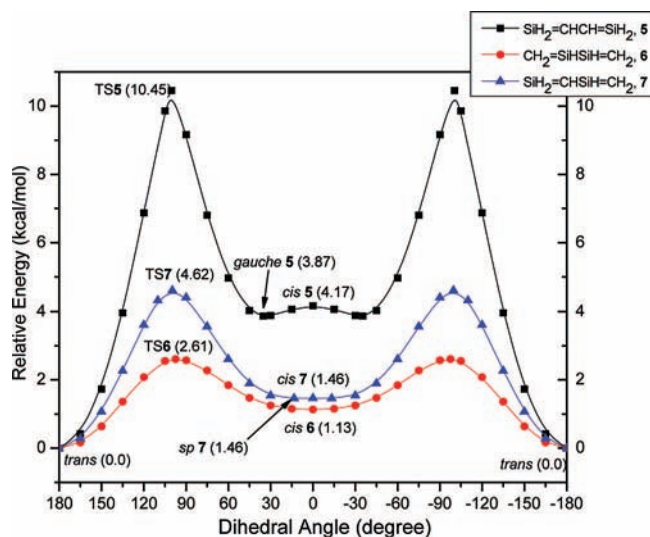


Figure 2. PESs for internal rotation of 1,4-disilabutadiene (**5**), 2,3-disilabutadiene (**6**), and 1,3-disilabutadiene (**7**). The energies (without ZPEs, kcal/mol) are relative to the *s*-trans rotamer.

4.4 [3.7] (**7**) > 4.0 [3.6] (**4**) > 2.6 [2.1] (**6**) (*s*-trans → *s*-cis). The barriers at CCSD(T)/cc-PVTZ are somewhat smaller than those at B3LYP/6-311+G(d,p), but the trends in both levels of calculations are the same, and the higher level calculations do not change our analysis or discussion. Because the differences between the B3LYP results and those at CCSD(T) are small, the B3LYP results are used as the basis for discussion. When larger systems are to be studied in the future, CCSD(T) calculations will not be possible, and comparisons with B3LYP will be the most relevant. The barriers for internal rotation in dienes having a C–C central bond (**3**, **5**, and **12**) are higher than those for dienes with a central Si–C bond (**4**, **7**). The smallest barrier is found in **6** with the long Si–Si central bond. It is interesting to note that silabutadienes **5** and **3** have a rotation barrier higher than that of 1,3-butadiene. The barrier heights for the backwards rotations (*gauche* → *s*-trans) are (kcal/mol) 6.2 (**5**), 4.3 (**3**), 3.1 (**12**), 3.1 (**7**), 2.3 (**4**), and 1.5 (**6**) (*s*-cis → *s*-trans). The relatively small barriers for the *gauche* → *s*-trans rotational processes for **4** and **6** imply that their *gauche* conformers are kinetically unstable with regard to rotation.

b. PESs of Di-, Tri-, and Tetrasilabutadienes, 8–11. This group of silabutadienes have either one or two Si=Si double bonds. The PESs (at B3LYP/6-311+G(d,p)) for internal rotation

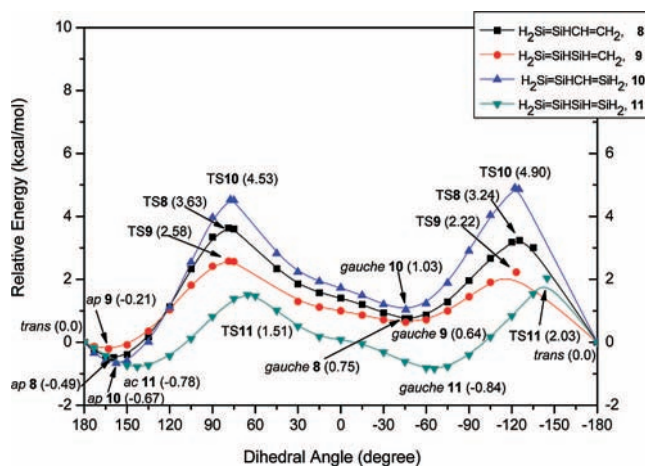


Figure 3. PESs for internal rotation of 1,2-disilabutadiene (**8**), 1,2,3-trisilabutadiene (**9**), 1,2,4-trisilabutadiene (**10**), and tetrasilabutadiene (**11**). The energies (without ZPEs, kcal/mol) are relative to the *s*-trans rotamer.

of silabutadienes **8–11** are shown in Figure 3. The PESs of **8–11** have the same general shape, but this shape is different from that calculated for silabutadienes **3–7** and that of 1,3-butadiene. The most pronounced difference is that the PESs of **8–11** are not the same between $\theta = 180$ to 0° and between $\theta = 0$ to -180° . On these PESs, we located ap (ac for **11**) and *gauche* conformers, as well as two different transition states. The *s*-cis conformers ($\theta = 0^\circ$) are not minima on these PESs. The global minimum for **8–10** is the ap rotamer, whereas for tetrasilabutadiene (**11**), it is the *gauche* conformer, but the ac rotamer is only slightly higher in energy. The energies of the ap (ac for **11**) structures are slightly lower than those of the *s*-trans ($\theta = 180^\circ$) minima; their geometries are almost the same as those of the *s*-trans conformers, except for the SiSiM¹M² (M = C, Si) dihedral angles which are 159.4, 162.9, 157.5, and 142.8°, (154.2, 155.9, 150.9, and 131.4° at MP2) for **8–11**, respectively (Table 3). The *gauche* conformers are located at $\theta = -48.1, -45.6, -45.7,$ and -65.6° , respectively (Table 3). The transition states which lead from the ap to the *gauche* conformers (TS(*t*-*g*)) are located at $\theta = 78.8, 78.7, 77.4,$ and 65.4° for **8–11**, respectively. The second TS, TS(*g*-*t*), is located between the *gauche* and *s*-trans rotamers (Figure 3) at θ values of $-125.5, -123.1, -122.^\circ,$ and -144.8° , respectively (Table 3).

For **8–11**, the rotation barriers, TS(*t*-*g*), relative to the ap rotamers follow the trend (kcal/mol, in brackets relative to *s*-trans, in italics at CCSD(T)/cc-PVTZ//B3LYP/6-311+G(d,p)) 4.9 [4.4, 3.3] (**10**) > 3.9 [3.5, 2.9] (**8**) > 2.7 [2.6, 1.8] (**9**) > 2.4 [1.8, 0.84] (**11**). As for **3–7**, also for **8–11**, the differences between the CCSD(T) and B3LYP rotation barriers are small. Because the PES is not symmetric around $\theta = 0^\circ$, the TS(*g*-*t*) barriers, leading from *s*-trans at $\theta = -180^\circ$ to *gauche*, have to be considered; these barriers (relative to *s*-trans) are (kcal/mol) 4.7 (**10**), 3.1 (**8**), 2.2 (**9**), and 2.1 (**11**). The barrier heights for the *gauche* → TS(*t*-*g*) → ap rotations are of 3.3 (**10**), 2.7 (**8**), 2.4 (**11**), and 1.8 (**9**) kcal/mol, respectively, and those for the *gauche* → TS(*g*-*t*) → *s*-trans ($\theta = -180^\circ$) rotations of 3.6 (**10**), 2.6 (**11**), 2.3 (**8**), and 1.4 (**9**) imply that the *gauche* conformers of **8–10** are kinetically less stable than the ap or *s*-trans conformers. In contrast, for **11**, the *gauche* conformer is kinetically more stable than the ap or *s*-trans conformers.

In summary, the highest barriers for internal rotation occur in silabutadienes possessing a central C–C bond (kcal/mol), that is, **5** (10.0) > **3** (7.4) ≥ **12** (7.0); the rotation barriers are

smaller for silabutadienes with the longer Si–C bond, that is, **10** (4.4) \approx **7** (4.4) \geq **8** (3.5). Silabutadienes that have a central Si–Si bond (which is longer than a C–Si or a C–C bond) have the smallest internal rotation barriers, that is, **6** (2.6) \approx **9** (2.6) $>$ **11** (1.8). The C–C, C–Si and Si–Si bond lengths in CH₃–CH₃, CH₃–SiH₃, and SiH₃–SiH₃ are 1.531, 1.885, and 2.354 Å, respectively (B3LYP/6-311+G(d,p)). Thus, a major factor controlling the height of the barrier for internal rotation in silabutadienes is the central M²–M³ single bond length. A shorter central bond increases the π – π overlap and the degree of π -conjugation in the diene and thus also the rotation barrier.³¹ A detailed discussion of the degree of π -conjugation and its relation to the internal rotation barrier is given below.

II. Geometries. The main geometric parameters (optimized at B3LYP and in some cases also at MP2, CCSD) of the stationary points on the PESs of silabutadienes **3–7** and of 1,3-butadiene are given in Table 2, and those of silabutadienes **8–11** are given in Table 3.

In general, the variations in the bond lengths upon rotation (changing θ) have similar trends in all dienes. Upon rotation from s-trans to the TS, the double bonds shorten, whereas the central single bonds lengthen. In the gauche rotamers, the bond lengths return nearly to the values of the s-trans rotamers (Table 2). For example, in 1,4-disilabutadiene (**5**), $r(\text{Si}=\text{C})$ shortens from 1.742 Å (s-trans) to 1.722 Å in TS (t-g), and it increases to 1.739 Å in the gauche conformer (1.740 Å in s-cis); concurrently, $r(\text{C}–\text{C})$ elongates from 1.428 Å (s-trans) to 1.475 Å (TS) and is finally shortened to 1.435 Å in s-cis (Table 2). The central single bonds are the shortest in the s-trans conformers.

In the s-trans minima of silabutadienes **3–7** and in the gauche (**3**), sp (**4** and **7**), and s-cis (**6**) rotamers, the doubly bonded fragments (CH₂=CH–, SiH₂=CH–, and CH₂=SiH–) are planar. In the s-trans and gauche rotamers of **8–11**, the Si=C double bonds are planar, but the external Si=Si double bonds are pyramidal around the silicon atoms (Table 3). The sum of the angles around the terminal Si¹ atoms (denoted as $\Sigma\alpha$) in the s-trans rotamers of **8**, **9**, **10**, and **11** are 345.9, 353.0, 337.0, and 352.0°, respectively (Table 3).

The Si=C bond lengths in the s-trans conformers of **3–7**, **9**, and **10** range from 1.742 to 1.710 Å, and the C=C bond lengths in **3** and **4** are 1.345 and 1.340 Å, respectively (Table 2). These bonds are longer than those in silene and ethylene (1.708 and 1.329 Å) respectively. The lengths of the central C–C bond in the s-trans conformers of **3** and **5** are 1.445 and 1.428 Å, respectively (Table 2), considerably shorter than that in ethane (1.531 Å) and slightly shorter than that in 1,3-butadiene (1.456 Å). The central Si–C bond lengths in **4**, **7**, **8**, and **10** of 1.845, 1.818, 1.850, and 1.820 Å, respectively (Table 2), are shorter than that in methylsilane (1.885 Å).^{32a} The central Si–Si bond in the s-trans, ap, and gauche minima of **6**, **9**, and **11** is shorter than that in H₃Si–SiH₃ (Tables 2 and 3), and $r(\text{Si}=\text{Si})$ in these rotamers is longer than that of SiH₂=SiH₂ (Tables 2 and 3).

The lengthening of the double bonds and shortening of the single bonds in the dienes relative to the corresponding monoenes and the corresponding singly bonded analogues implies the existence of π -conjugation in the studied silabutadienes. The degree of π -conjugation in silabutadienes is discussed in Section III.

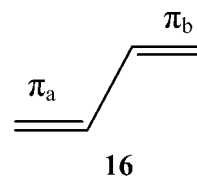
The calculated Si₁Si₂Si₃Si₄ angle of the gauche rotamer of **11** of -65.6° is between the angles found experimentally for **1** (51°)^{2a} and for **2a** (72°).^{3a} The calculated $r(\text{Si}=\text{Si})$ in **11** (2.187 Å) is between the experimentally determined values for **1** (2.175 Å),^{2a} **2a** (2.200 and 2.198 Å)^{3a} and **2b** (2.198 and 2.217 Å).^{3b}

$r(\text{Si}–\text{Si})$ of **11** (2.302 Å) is slightly shorter than that measured for **1**, **2a**, and **2b** (2.321,^{2a} 2.338,^{3a} and 2.340 Å,^{3b} respectively).^{32b} The small differences between theory and experiment may result from the bulky substituents present in the experimental systems.

III. π -Conjugation in s-trans Conformers. An important property of polyenes is the existence of π -conjugation between their vicinal multiple bonds.³³ A significant outcome of π -conjugation is that the reactivity of each of the double bonds in the π -network depends on changes throughout the conjugated system exhibiting remote chemical control. Evidence for its existence can be found by its manifestations in molecular structure.^{33,34} In the following sections, we study the extent of π -conjugation in the studied silabutadienes and correlate π -conjugation with s-trans \rightarrow gauche internal rotation barriers.

The extent of π -conjugation in the s-trans silabutadienes will be estimated by using the following criteria: (a) REs calculated by using the NBO^{12,13} and BLW methods¹⁴ as well as from the degree of electron delocalization, (b) bond separation energies, and (c) molecular structures.

a. NBO and BLW Estimates of π -Conjugation. π -Conjugation stabilization energies (also being referred to as quantum-mechanical RE, QMRE)¹³ were evaluated by calculating the NBO donor–acceptor stabilizing interactions between the conjugated π_a and π_b double bonds (see **16**).



The ideal localized Lewis structure in which exactly two π -electrons reside in each of the π -bonds is distorted because of π -conjugation by donor–acceptor interactions of the type $\pi_a \rightarrow \pi_b^*$ and $\pi_b \rightarrow \pi_a^*$. These interactions lead to $\pi_a \rightarrow \pi_b^*$ and $\pi_b \rightarrow \pi_a^*$ charge delocalization and to a perturbative correction to the zero-order natural Lewis-structure wave functions. According to perturbation theory the stabilization due to $\pi_a \rightarrow \pi_b^*$ interaction is given by eq 1, where $\Delta\varepsilon$ is the energy difference between the interacting π and π^* orbitals and $\langle \pi_a | \hat{F} | \pi_b^* \rangle$ is the Fock matrix element between these orbitals. The size of $\langle \pi_a | \hat{F} | \pi_b^* \rangle$ and its variation with distance and spatial orientation can be visualized in terms of the overlap between π_a and π_b^* .¹³

$$\Delta E(\pi_a \rightarrow \pi_b^*) = -2 \frac{\langle \pi_a | \hat{F} | \pi_b^* \rangle^2}{\Delta\varepsilon} \quad (1)$$

In NBO terms, the strength of π -conjugation is described by the sum of the stabilization energies $\Delta E(\pi_a \rightarrow \pi_b^*) + \Delta E(\pi_b \rightarrow \pi_a^*)$ ($\equiv A$ for the s-trans conformers and B for the TSs) and by the charge transfer from π_a to π_b^* .¹³ The conjugative stabilization energies $\Delta E(\pi_a \rightarrow \pi_b^*)$ and $\Delta E(\pi_b \rightarrow \pi_a^*)$, $\Delta\varepsilon$, $\langle \pi_a | \hat{F} | \pi_b^* \rangle$ ($\equiv F_{ab^*}$) and $\langle \pi_b | \hat{F} | \pi_a^* \rangle$ ($\equiv F_{ba^*}$) values for dienes **3–12**, as well as the destabilization energies caused by deleting F_{ab^*} and F_{ba^*} from the Fock matrix, are given in Table 4, and the occupancies of the π_a , π_b , π_a^* , and π_b^* NBOs are given in Table 5.

For dienes **3–12**, the conjugative stabilization energies A range from 10.1 to 49.6 kcal/mol. The sum of the conjugative stabilization energies in the transition states for internal rotation (B) are considerably smaller, ranging from 0.06 to 3.64 kcal/

TABLE 4: π -Conjugation Stabilization Energies ($\Delta E[\pi_a \rightarrow \pi_b^*]$ and $\Delta E[\pi_b \rightarrow \pi_a^*]$), $\Delta\epsilon$ ($\pi_a \rightarrow \pi_b^*$ and $\pi_b \rightarrow \pi_a^*$), $\langle \pi_a | \hat{F} | \pi_a^* \rangle$, $\langle \pi_b | \hat{F} | \pi_b^* \rangle$, and $\langle \pi_b | \hat{F} | \pi_a^* \rangle$ for the s-trans Rotamers and TSs (TS(t-g) or TS(g-c)) of **3–12** and their Internal Rotation Barriers

diene	s-trans rotamers				TS(t-g) or TS(g-c)				rotation barrier ^{e,c}		
	π_a	π_b	deletion energy ^{a,c}	ΔE^d [$\pi_a \rightarrow \pi_b^*$]	ΔE^d [$\pi_b \rightarrow \pi_a^*$]	ΔE^d [$\pi_a \rightarrow \pi_b^*$]	ΔE^d [$\pi_b \rightarrow \pi_a^*$]	$\Delta\epsilon^d$ [$\pi_a \rightarrow \pi_b^*$]		$\Delta\epsilon^d$ [$\pi_b \rightarrow \pi_a^*$]	
$H_2C=CH-HC=CH_2$ (12)	15.07	15.07	30.1	0.31	0.31	0.061	1.08	0.35	0.017	0.017	6.6
$H_2Si=CH-HC=CH_2$ (3)	22.60	15.11	37.7	0.27	0.24	0.070	2.13	0.33	0.024	0.019	7.4
$H_2C=SiH-HC=CH_2$ (4)	5.76	8.12	13.9	0.24	0.29	0.033	0.12	0.25	0.005	0.007	4.0
$H_2Si=CH-HC=SiH_2$ (5)	24.81	24.81	49.6	0.20	0.20	0.063	1.82	0.24	0.019	0.019	10.0
$H_2C=SiH-HSi=CH_2$ (6)	5.05	5.05	10.1	0.22	0.22	0.030	0.03	0.22	0.002	0.002	2.6
$H_2Si=CH-HSi=CH_2$ (7)	12.82	5.78	18.6	0.26	0.18	0.052	0.46	0.26	0.010	0.005	4.4
$H_2Si=SiH-HC=CH_2$ (8)	7.18	7.84	15.0	0.23	0.24	0.036	0.02	0.24	0.002	0.001	3.5 (3.9)
$H_2Si=SiH-HSi=CH_2$ (9)	6.95	4.96	11.9	0.21	0.17	0.034	0.11	0.21	0.004	0.000	2.6 (2.7)
$H_2Si=SiH-HC=SiH_2$ (10)	6.59	14.13	20.7	0.17	0.20	0.030	0.02	0.20	0.002	0.005	4.4 (4.9)
$H_2Si=SiH-HSi=SiH_2$ (11)	7.47	7.47	14.9	0.16	0.16	0.031	0.01	0.16	0.001	0.001	1.8 (2.4)

^a In kcal/mol. ^b $\Delta E[\pi_a \rightarrow \pi_b^*] + \Delta E[\pi_b \rightarrow \pi_a^*]$. ^c Destabilization energy due to the deletion of $\langle \pi_a | \hat{F} | \pi_b^* \rangle$ and $\langle \pi_b | \hat{F} | \pi_a^* \rangle$ Fock matrix elements. ^d $\Delta\epsilon$, $\langle \pi_a | \hat{F} | \pi_b^* \rangle$ and $\langle \pi_b | \hat{F} | \pi_a^* \rangle$ in Hartrees. ^e Relative to the s-trans rotamer; in parenthesis, relative to the lowest energy rotamer.

mol. The large difference between *A* and *B* indicates the disruption of π -conjugation upon rotation to the TSs in which the mutual orientation of the π and π^* orbitals prevents effective π -overlap.

According to the degree of π -conjugation, the studied silabutadienes can be divided into three groups: (a) dienes with a central C–C bond have the largest degree of π -conjugation (kcal/mol), **5** (49.6) > **3** (37.7) > **12** (30.1); (b) silabutadienes with a Si–C central bond have a smaller, yet large, degree of π -conjugation, **10** (20.7) > **7** (18.6) > **8** (15.0) > **4** (13.9); and (c) silabutadienes with a central Si–Si bond have the smallest degree of π -conjugation **11** (14.9) > **9** (11.9) > **6** (10.1). Deletion of F_{ab^*} and F_{ba^*} leads to somewhat smaller stabilization energies, but the trends discussed above remain the same (Table 4). The trends in π -conjugation listed above are caused mainly by the decrease in the overlap between π_a and π_b^* and between π_b and π_a^* NBOs when the central single bond becomes longer^{31,35} (e.g., representative bond lengths in the localized structures (Table 6) are C–C, (1.542 Å (**5**)) < Si–C (1.866 Å (**10**)) < Si–Si (2.356 Å (**11**)). The trend within each of the three groups is affected by a combination of the energy difference between the π and π^* orbitals ($\Delta\epsilon$), the polarities of the individual π and π^* orbitals and small differences in the central single bond length which affect the orbitals' overlap. For example, the overlap (*S*) between the preorthogonal π and π^* NBOs (PNBO) in 1,3-butadiene is larger than that in **5** (0.222 vs 0.208, respectively), but $\Delta\epsilon$ in **5** is significantly smaller than that of 1,3-butadiene (0.20 vs 0.31 hartree, respectively, Table 4), resulting in a stronger π -conjugation in **5**. The large difference in conjugative stabilization energy between the two isomeric disilabutadienes **5** (49.6 kcal/mol) and **6** (10.1 kcal/mol) is a good example of the factors which determine conjugative stabilization. Both have two C=Si bonds, but, in **5**, the two C=Si bonds are interconnected by a C–C bond, whereas in **6**, they are interconnected by the longer Si–Si bond, resulting in a smaller overlap (*S*) between the π and π^* PNBOs of **6** relative to that of **5** (0.178 and 0.208, respectively), as shown schematically in Figure 4a,b. The differences in the overlap of the orbitals is also manifested in the much larger F_{ab^*} and F_{ba^*} of **5** relative to **6** (Table 4).³⁵ In addition, $\Delta\epsilon$ of **5** is smaller than that of **6**. Thus, the larger overlap and Fock matrix elements and a smaller energy difference between the π and π^* orbitals in **5** lead, according to eq 1, to its significantly larger degree of π -conjugation. Note that the strength of π -conjugation in 1,3-disilabutadienes **5** and in 1-silabutadiene **3** is larger than that in 1,3-butadiene, suggesting a more effective remote chemical control and possible transfer of chemical and electronic information in specifically designed silapolyenes relative to polyacetylene. This interesting possibility will be explored in future studies.

The occupancies of the π_a^* and π_b^* NBO orbitals of silabutadienes **3–11** (s-trans rotamers) range from 0.041 to 0.166 electrons; occupancies of the π^* NBOs of the TSs are much smaller, between 0.001 to 0.038 electrons. The trend in the occupancies of the π^* orbitals, which give the degree of electron delocalization, parallels the conjugative stabilization energies. Accordingly, the largest electron delocalization is found in 1,4-disilabutadiene **5** (0.17 electron in π_a^* and π_b^*), which also exhibits the largest conjugative stabilization energy *A* (49.6 kcal/mol, Tables 4 and 5), whereas the smallest electron delocalization is calculated for 2,3-disilabutadiene **6** (0.042 el.; *A* = 10.1 kcal/mol).

The degree of π -conjugation was also calculated by using the BLW method (for details, see the Methods of Calculation

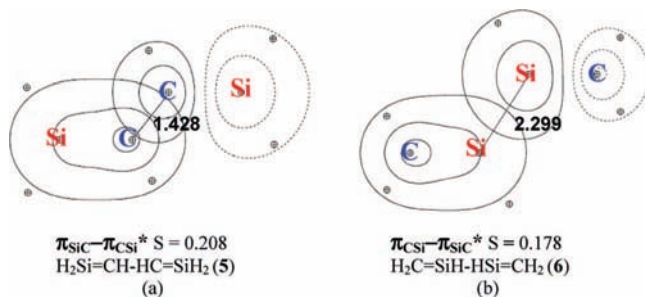
TABLE 5: Electron Occupancy (Electrons) of the π_a , π_b , π_a^* , and π_b^* NBOs of the *s-trans* Rotamer and of the TSs for Internal Rotation of Dienes 3–12

diene	occupancy in <i>s-trans</i> NBOs				occupancy in TS NBOs			
	π_a	π_b	π_a^*	π_b^*	π_a	π_b	π_a^*	π_b^*
H ₂ C=CH–HC=CH ₂ (12)	1.925	1.925	0.073	0.073	1.981	1.981	0.020	0.020
H ₂ Si=CH–HC=CH ₂ (3)	1.876	1.906	0.091	0.120	1.967	1.976	0.025	0.034
H ₂ C=SiH–HC=CH ₂ (4)	1.958	1.949	0.046	0.041	1.990	1.976	0.008	0.008
H ₂ Si=CH–HC=SiH ₂ (5)	1.829	1.829	0.166	0.166	1.960	1.960	0.038	0.038
H ₂ C=SiH–HSi=CH ₂ (6)	1.955	1.955	0.042	0.042	1.978	1.978	0.005	0.005
H ₂ Si=CH–HSi=CH ₂ (7)	1.913	1.942	0.057	0.080	1.961	1.986	0.009	0.015
H ₂ Si=SiH–HC=CH ₂ (8)	1.927	1.945	0.066	0.055	1.966	1.974	0.026	0.010
H ₂ Si=SiH–HSi=CH ₂ (9)	1.925	1.950	0.058	0.063	1.958	1.975	0.019	0.007
H ₂ Si=SiH–HC=SiH ₂ (10)	1.892	1.885	0.130	0.076	1.955	1.955	0.033	0.012
H ₂ Si=SiH–HSi=SiH ₂ (11)	1.922	1.922	0.075	0.075	1.949	1.949	0.024	0.024

TABLE 6: REs Calculated by BLW and Bond Separation Reactions and Internal Rotation Barriers (All in kcal/mol)

diene	BLW ^{a,b}		bond separation energies ^c		rotation barrier ^{c,d}
	ARE	VRE	eq 2	eq 3 ^e	
H ₂ C=CH–HC=CH ₂ (12)	12.4	14.4	14.5	9.2 (7.4)	6.6
H ₂ Si=CH–HC=CH ₂ (3)	15.9	18.9	14.0	11.7 (9.1)	7.4
H ₂ C=SiH–HC=CH ₂ (4)	7.1	7.6	5.0	4.7 (3.8)	4.0
H ₂ Si=CH–HC=SiH ₂ (5)	21.3	26.7	15.0	15.5 (12.2)	10.0
H ₂ C=SiH–HSi=CH ₂ (6)	4.8	5.2	6.0	4.5 (4.2)	2.6
H ₂ Si=CH–HSi=CH ₂ (7)	10.1	11.0	11.1	7.7 (6.4)	4.4
H ₂ Si=SiH–HC=CH ₂ (8)	7.9	8.6	3.5	4.7 (3.1)	3.5
H ₂ Si=SiH–HSi=CH ₂ (9)	6.1	6.7	7.9	5.1 (4.2)	2.6
H ₂ Si=SiH–HC=SiH ₂ (10)	11.5	12.7	10.2	8.2 (6.2)	4.4
H ₂ Si=SiH–HSi=SiH ₂ (11)	7.5	8.4	9.4	5.3 (4.1)	1.8

^a For planar *s-trans* conformation. ^b Obtained by using GAMESS, at B3LYP/6-311G(d,p), B3LYP uses VWN5. ^c At B3LYP/6-311+G(d,p). ^d About the central single bond, relative to the *s-trans* structure. ^e The M¹M²M³M⁴ dihedral angles in H₂M¹=M²H–M³H₂–M⁴H₃ and H₃M¹–M²H₂–M³H–M⁴H₂ are constrained to 180.0°; energies in parenthesis use the energies of the fully optimized butenes.

**Figure 4.** Preorthogonal NBOs (PNBO) contours drawn 0.8 Å above the molecular plane showing the π_a – π_b^* overlap in the *s-trans* conformers of (a) **5** and (b) **6**.

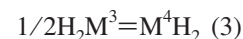
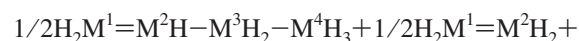
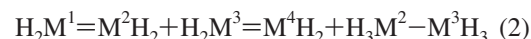
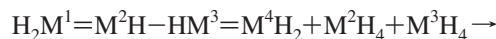
section).¹⁴ By using this method, which localizes two π -electrons on each of the individual double bonds, we have calculated the AREs (the geometry of the localized state is also optimized) and VREs (by using the geometry of the delocalized structure) which are presented in Table 6.

The VRE follow the trend (kcal/mol) **5** (26.3) > **3** (18.9) > **12** (14.4) > **10** (12.7) > **7** (11.0) > **8** (8.6) \geq **11** (8.4) > **4** (7.6) > **9** (6.7) > **6** (5.2). These REs are significantly smaller than the NBO π -conjugation stabilization energies^{36a} (Table 4), but the trend with both methods is the same,^{36b} lending additional confidence in our conclusions regarding the relative degree of π -conjugation in these molecules.

c. Bond Separation Energies. Bond separation reactions in which the conjugated π -bonds are separated from each other, thus disrupting conjugation, are a common tool for estimating

the degree of resonance interactions in conjugated systems.³⁷ A variety of reaction types, for example, isodesmic (eq 2), homodesmotic, and hypohomodesmotic, were used for estimating REs of conjugative systems resulting in a widespread of energies (see ref 38 and references cited therein for a critical evaluation of the various types of bond-separation energies). The main difficulty with such reactions is that they depend on reference compounds and that they suffer from imbalance in the bond environment and bond types on the two sides of the equations.

For estimating the π -REs of silabutadienes and 1,3-butadiene, we use isodesmic eq 2 (suggested in ref 38) and 3.



In eq 2, the diene is separated into the three fragments from which it is composed, two double bonds and a single bond that connects them. The main difficulty with eq 2 is that the hybridization on both sides of the equation is imbalanced; for example, a M(sp²)–M(sp²) single bond on the left side of the equation is compared to a M(sp³)–M(sp³) single bond on the right side of the equation (for a more detailed discussion of this problem, see ref 38). In eq 3, we compare the hydrogenation energy of each of the double bonds in the conjugated molecules to the hydrogenation of the same double bond in the nonconjugated ethene or sila-ethene. This equation suffers from unbalanced hybridization on both sides and also from an imbalance due to stabilization of the right side of the equation by hyperconjugative interactions, for example, between the M¹=M² π -bond with the $\sigma^*(\text{M}^3-\text{M}^4)$ orbital in H₂M¹=M²H–M³H₂–M⁴H₃. To overcome the later problem, we calculated eq 3 by using H₂M¹=M²H–M³H₂–M⁴H₃ and H₃M¹–M²H–M³H–M⁴H₂, in which the $\angle\text{M}^1\text{M}^2\text{M}^3\text{M}^4$ dihedral angle is constrained to 180° (which is not a minimum), thus deactivating hyperconjugation (which is effective when the M¹M²M³M⁴ dihedral angle is 60–120°). The energies of eqs 2 and 3 for silabutadienes **3–11** and for 1,3-butadiene are given in Table 6 (for eq 3, we also give the reaction energies obtained by using the optimal structures of the butenes).

The REs calculated by eqs 2 and 3 are somewhat smaller than those calculated by using the BLW method and significantly smaller than the NBO REs. However, the energies calculated

TABLE 7: Bond Lengths in Delocalized and Localized Silabutadienes (3–11) and in 1,3-butadiene (12) and the Relative Change in the Bond Lengths of Delocalized versus Localized Structures (BLW) and in the TSs versus those in the s-trans Rotamer^a

	delocalized ^{b,c}			localized ^{b,d}			$\Delta r(\text{delocalized} - \text{localized})/$ $r(\text{delocalized})^{b,d,e}$			$\Delta r(\text{s-trans} - \text{TS})/$ $r(\text{s-trans})^{e,f}$		
	M ¹ =M ²	M ² -M ³	M ³ =M ⁴	M ¹ -M ²	M ² -M ³	M ³ =M ⁴	M ¹ =M ²	M ² -M ³	M ³ =M ⁴	M ¹ =M ²	M ² -M ³	M ³ =M ⁴
H ₂ M ¹ =HM ² -M ³ H=M ⁴ H ₂												
H ₂ C=CH-HC=CH ₂ (12)	1.338	1.457	1.338	1.326	1.527	1.326	0.9	-5	0.9	0.4	-2	0.4
H ₂ Si=CH-HC=CH ₂ (3)	1.730	1.447	1.344	1.713	1.534	1.326	1	-6	1	0.6	-3	0.8
H ₂ C=SiH-HC=CH ₂ (4)	1.709	1.848	1.338	1.704	1.895	1.330	0.3	-3	0.6	0.1	-1	0.2
H ₂ Si=CH-HC=SiH ₂ (5)	1.744	1.427	1.744	1.714	1.542	1.714	2	-8	2	1	-3	1
H ₂ C=SiH-HSi=CH ₂ (6)	1.719	2.302	1.719	1.713	2.357	1.713	0.4	-2	0.4	0.1	-1	0.1
H ₂ Si=CH-HSi=CH ₂ (7)	1.721	1.822	1.713	1.710	1.878	1.703	0.6	-3	0.6	0.4	-1	0.2
H ₂ Si=SiH-HC=CH ₂ (8)	2.149	1.848	1.340	2.140	1.904	1.330	0.4	-3	0.7	-0.1	-2	0.4
H ₂ Si=SiH-HSi=CH ₂ (9)	2.155	2.290	1.717	2.145	2.354	1.710	0.5	-3	0.4	0	-1	0.1
H ₂ Si=SiH-HC=SiH ₂ (10)	2.156	1.817	1.725	2.140	1.886	1.709	0.7	-4	0.9	0.8	-2	0.6
H ₂ Si=SiH-HSi=SiH ₂ (11)	2.157	2.279	2.157	2.144	2.356	2.144	-0.6	-3	0.6	0.7 ^g	-2	0.7 ^g

^a Bond length in Å. ^b Calculated for planar structures by using B3LYP (VWN5)/6-311G(d,p). ^c The bond lengths for 3–7, 11, and 12 are very similar to those given in Tables 2 and 3. The M¹=M² bond length of 8–10 are shorter than those calculated for the non-planar structures (see Table 3). ^d Optimized by using the block localized wave function (BLW). ^e In %. ^f Calculated by using the bond lengths given in Tables 2 and 3. ^g s-trans and TS in C₂ symmetry.

bonds are pyramidal (the planarization energy is however small, e.g., in 11, it is only 1.4 kcal/mol). The results of these comparisons are presented in Table 7.

The data in Table 7 show that, in the delocalized s-trans conformers the shortening of the single bonds is larger than the lengthening of the double bonds by a factor of 4–5. The largest shortening and elongation occur in 1,4-disilabutadiene 5 (C–C (-8%) and Si=C (2%)). We also observe that the changes in the bond lengths in the TS versus the s-trans structure are smaller than the corresponding differences between the localized and delocalized structures (e.g., in the case of 5, C–C (-3%), Si=C (1%)). This results from the contributions of hyperconjugative interactions which are present in the transition states but not in the s-trans conformer (see section III.d) and from residual π -delocalization. We therefore conclude that the effect of π -conjugation on structure is better estimated by a direct comparison of the calculated structures of strictly localized and delocalized dienes rather than from comparison of structures along the internal rotation coordinate.

Examination of Table 7 shows that the degree of shortening of the central M²-M³ single bond follows the order 5 > 3 > 12 > 10 \geq 4 \approx 7 \approx 8 \approx 9 \approx 11 > 6.^{43a} The structure of 1,4-disilabutadiene 5 is the most affected by delocalization, and that of 2,3-disilabutadiene 6 is the least affected. This trend in the M²-M³ bond length shortening is very similar to the trend in rotation barriers which is (kcal/mol) 5 (10.0) > 3 (7.4) > 12 (6.6) > 10 \approx 7 (4.4) \geq 4 (4.0) \geq 8 (3.5) > 9 \approx 6 (2.6) > 11 (2.4),^{43b} indicating that π -conjugation is a major contributor to both the changes in bond lengths and the height of the barriers for internal rotation. As pointed above, both trends are controlled by the length of the M²-M³ central bond, conjugation being the largest for a central C–C bond (5) and the smallest for a central Si–Si bond (6).³¹

d. Strength of π -Conjugation and Rotation Barriers. Figure 5 presents the correlation found between π -conjugation energies, calculated by using the various methods discussed above, and the barriers for internal rotation around the central M²-M³ bond in all silabutadienes. There is a fairly good linear correlation between REs and the internal rotation barriers, indicating that internal rotation barriers in dienes are determined by the strength of π -conjugation. However, the slopes of the correlation lines show that VREs and AREs are more than twice larger than the internal rotation barriers, those calculated by using NBO are ca. 4–5 times larger, and REs calculated by eq 3 are ca. 1.5 times larger than the

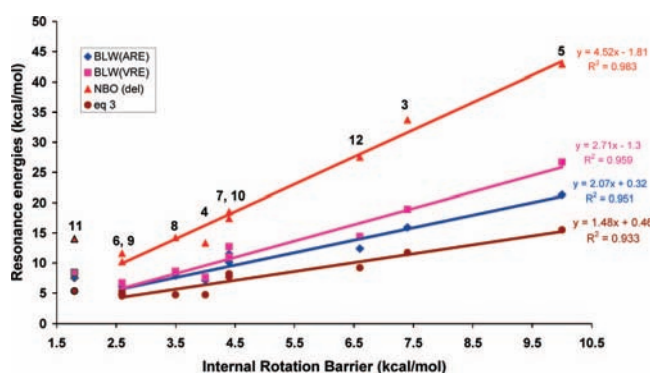
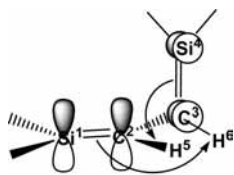


Figure 5. Correlation between the calculated REs of 3–11 and the internal rotation barrier (relative to the s-trans rotamer). Tetrasilabutadiene 11 is not included in the correlation.

internal rotation barriers. Thus, barriers for internal rotation do not reflect the full π -RE. Although the stabilization by π -conjugation is essentially deactivated in the transition state because of the lack of π - π^* overlap, other stabilizing interactions which do not exist in the conjugated s-trans dienes come into effect in the TS and partly compensate for the loss of π -conjugation. For example, in the TS for internal rotation in 5, four significant stabilizing interactions, which do not occur in the s-trans conformer, are present: $\pi(\text{Si}^1=\text{C}^2) \rightarrow \sigma^*(\text{C}^3-\text{H}^6)$, $\sigma(\text{C}^3-\text{H}^6) \rightarrow \pi^*(\text{Si}^1=\text{C}^2)$, $\pi(\text{C}^3=\text{Si}^4) \rightarrow \sigma^*(\text{C}^2-\text{H}^5)$, and $\sigma(\text{C}^2-\text{H}^5) \rightarrow \pi^*(\text{C}^3=\text{Si}^4)$ (these interactions are depicted schematically in 17). The sum of second-order perturbation stabilization energies of these four interactions is 21.4 kcal/mol, almost half of the value of the π - π^* conjugative interaction in the s-trans rotamer (42.9 kcal/mol, Table 4). There are also other less significant stabilizing conjugation interactions which come into effect in the TS and do not occur in the s-trans conformer, for example, $\pi(\text{Si}^1=\text{C}^2) \rightarrow \sigma^*(\text{C}^3-\text{Si}^4)$ and $\pi(\text{Si}^3=\text{C}^4) \rightarrow \sigma^*(\text{C}^1-\text{Si}^2)$, which only contribute 1.28 kcal/mol each to the stabilization of the TS, stabilizing the TS even more and leading to an internal rotation barrier that is less than half of the RE, in agreement with the slopes of VRE and ARE versus rotation barrier curves shown in Figure 5. To test the total difference in the conjugative stabilization between the s-trans and TS conformers of 5, we have also performed for both a NOSTAR¹² NBO calculation in which all the non-Lewis, Rydberg, and antibond NBOs are deleted, resulting in an idealized NBO Lewis structure, with all Lewis NBOs doubly

occupied. In other words, this deletion deactivates all conjugative stabilizations. The deletion energy is the energy difference between an electronic structure in which electron delocalization exists and the fully localized ideal Lewis structure, that is, the total stabilization energy due to both π -conjugation and hyperconjugation. The NOSTAR deletion energies show that the *s*-trans conformer of **5** is stabilized by conjugation by 23.1 kcal/mol more than its TS. The absence of π - π^* conjugation in the TS should have led to a difference of 42.9 kcal/mol (Table 4). The much smaller difference of 23.1 kcal/mol calculated with the NOSTAR deletion procedure results from stabilizing hyperconjugation interactions that are absent in *s*-trans conformer but exist in the TS because of proper orientation of, for example, the $\pi(\text{Si}=\text{C})-\sigma^*(\text{C}-\text{H})$ orbitals (see **17**) and other smaller contributions. In conclusion, new hyperconjugative interactions which arise upon rotation to the TS stabilize the TS and lower the internal rotation barrier relative to the value expected from the disruption of the π - π^* conjugation. A question that arises is why the NBO REs are four times larger than the internal rotation barriers, when, on the basis of conjugation and hyperconjugation alone (e.g., for **5**), it should be only twice as large. Are steric effects responsible? Are other effects involved?⁴⁶ These questions remain to be answered in future research.

An important conclusion from this analysis is that rotation barriers are not an accurate tool for approximating π -REs,⁴⁷ because factors such as differences between rotamers in hyperconjugation, steric congestion, and so forth, can reduce (or increase) the barrier significantly and complicate the interpretation. The ongoing vivid controversy regarding the origin of the rotation barrier in ethane demonstrates nicely the difficulty to relate the internal rotation barrier to a specific electronic and steric property.⁴⁸⁻⁵³ The barriers for internal rotation, however, do provide the correct trends in REs when comparing a series of compounds, such as the silabutadienes studied here.



17

Conclusions

The PESs of all possible silabutadienes (total of nine) were studied by using a variety of theoretical methods. The studied silabutadienes are 1-silabutadiene (**3**), 2-silabutadiene (**4**), 1,4-disilabutadiene (**5**), 2,3-disilabutadiene (**6**), 1,3-disilabutadiene (**7**), 1,2-disilabutadiene (**8**), 1,2,3-trisilabutadiene (**9**), 1,2,4-trisilabutadiene (**10**), and tetrasilabutadiene (**11**). The prototype 1,3-butadiene (**12**) was also studied for comparison. The main issues of interest are the barriers which separate the various rotamers on the PES and the degree of π -conjugation present in the *s*-trans conformers of each of the silabutadienes.

The PESs for internal rotation in silabutadienes **3**, **4**, **5**, and **7** and in 1,3-butadiene have a similar shape. The PES between $\theta = 180$ to 0° is a mirror image of the PES from $\theta = 0$ to -180° . Along these PESs, *s*-trans and *gauche* (or *sp*) minima exist, and two transition states, TS(*t*-*g*) and the *s*-*cis* conformer (TS(*g*-*g*)), connect these minima. In 2,3-disilabutadiene (**6**), the relatively long Si-Si central bond removes the steric congestion

that causes the other silabutadienes to distort from the *s*-*cis* conformer to *gauche*, so that **6** has two planar geometry minima, that is, *s*-*trans* and *s*-*cis*. For these five silabutadienes (**3-7**) and 1,3-butadiene, the *s*-*trans* conformers are the most stable rotamers.

The PESs for internal rotation of 1,2-disilabutadiene (**8**), 1,2,3-trisilabutadiene (**9**), 1,2,4-trisilabutadiene (**10**), and tetrasilabutadiene (**11**) are more complex than those of **3-7**. Their Si=Si double bonds are pyramidal around silicon throughout the entire course of internal rotation. For these silabutadienes, rotation from $\theta = 180$ to 0° and from $\theta = -180$ to 0° are not mirror images. Along these PESs, we find *ap* and *gauche* minima and two different transition states, TS(*t*-*c*) and TS(*g*-*t*). The most stable conformers are the *ap* conformers (**8-10**, with $M^1M^2M^3M^4$ dihedral angles of $157-163^\circ$), and for tetrasilabutadiene **11**, it is the *gauche* rotamer ($\angle\text{Si}^1\text{Si}^2\text{Si}^3\text{Si}^4 = -45.7^\circ$). The optimized structure of the *gauche* minima of tetrasilabutadiene **11** is in good agreement with the experimental structures of **1**^{2a} and **2a**.^{3a}

The internal rotation barriers around the central M^2-M^3 bond in $\text{H}_2M^1=M^2\text{H}-\text{HM}^3=M^4\text{H}_2$ depend primarily on the M^2-M^3 bond length.^{31,35} The barrier is the highest when the central bond is a C-C bond and the lowest when it is a Si-Si bond, and it follows the order (kcal/mol) **5** (10.0) > **3** (7.4) \geq **12** (7.0) (C-C), **10** (4.4) \approx **7** (4.4) \geq **8** (3.5) (Si-C), and **6** (2.6) \approx **9** (2.6) > **11** (1.8) (Si-Si).

π -Conjugative stabilization energies were calculated by using NBO and BLW methods as well as by bond-separation energies. The strength of π -conjugation is larger as the central single bond length is shorter because of better overlap of the π -conjugating orbitals. The trend in the degree of π -conjugation is similar with all methods, and it correlates linearly with the calculated internal rotation barriers. An interesting unexpected observation is that π -conjugation is larger in 1-silabutadienes (**3**) and in 1,4-silabutadiene (**5**) than in 1,3-butadiene **12**. The implications of this observation on their physical properties and chemistry remains to be explored.

NBO REs are in average twice larger than those calculated by using BLW or bond-separation energies, and they are in average 4.5 times larger than the internal rotation barriers. However, the important point is that the trends in the degree of π -conjugation, those that provide insight into and understanding of the differences in structural and chemical properties in a series of compounds, are very similar with all methods used.

A reasonably good linear correlation is observed between the internal rotation barriers and the degree of π -conjugation showing that π -conjugation plays an important role in determining the internal rotation barrier heights. However, the calculated π -REs are 2-4 times larger than the internal rotation barriers, implying that internal rotation barriers are a proper tool for estimating trends in REs but are not to be used for estimating absolute REs.

Future studies will investigate extended silapolyenes examining how extension of the polyenic chain affects their structures and electronic properties. Will such silapolyenes have similar properties or even superior ones to polyacetylenes?

Acknowledgment. We thank Professor F. Weinhold (Wisconsin) for advice and discussions and Prof. Y. Mo (Western Michigan) for providing us the software for performing BLW calculations. This research is supported by the Israel-USA binational science foundation (BSF) and by the Minerva foundation in Munich. H.-W. X. thanks the Israel Council for Higher Education for a Postdoctoral Fellowship.

Supporting Information Available: (1) Table S1: optimized Cartesian coordinates (B3LYP/6-311+G(d,p)), schematic ball-and-stick drawings of the stationary points on the PESs for internal rotation of silabutadienes **3–11** and their total energies. (2) Table S2: geometric parameters and total energies of tetrasilabutadiene **11** at the C_{2h} , C_2 , and C_i symmetries calculated at B3LYP, MP2, and CCSD with the 6-311+G(d,p) basis set. (3) Figure S1: preorthogonal NBO (PNBO) contours drawn 0.8 Å above the molecular plane showing the $\pi_a \rightarrow \pi_b^*$ overlap in the s-trans conformer of **3–11**. (4) Input file for BLW calculation of the s-trans conformer of **5**. This material is available free of charge via the Internet at <http://pubs.acs.org>.

References and Notes

- (1) (a) Weidenbruch, M. In *The Chemistry of Organic Silicon Compounds*; Rappoport, Z., Apeloig, Y., Eds.; John Wiley & Sons, 2001; Vol. 3, pp 391–428, Chapter 5. (b) Weidenbruch, M. In *Organosilicon Chemistry V: From Molecules to Materials*; Auner, N., Weis, J., Eds.; Wiley-VCH, 2003; p 114–125. (c) Tokitoh, N.; Okazaki, R. *Coord. Chem. Rev.* **2000**, *210*, 251. (d) Kira, M.; Iwamoto, T. *Adv. Organomet. Chem.* **2006**, *54*, 73. (e) Brook, M. A. In *Silicon in Organic, Organometallic, and Polymer Chemistry*; John Wiley & Sons, 2000; pp 39–96, Chapter 3. (f) Gaspar, P. P. In *Organosilicon Chemistry VI: From Molecules to Materials*; Auner, N., Weis, J., Eds.; Wiley-VCH, 2005; pp 10–24, Chapter 1. (g) Apeloig, Y. In *The Chemistry of Organic Silicon Compounds*; Patai, S., Rappoport, Z., Eds.; Wiley, 1989; pp 57–226, Chapter 2. (h) Apeloig, Y.; Karni, M. In *The Chemistry of Organic Silicon Compounds*; Rappoport, Z., Apeloig, Y., Eds.; John Wiley & Sons, 1998; Vol. 2, pp 1–101, Chapter 1. (i) Karni, M.; Apeloig, Y.; Kapp, J.; Schleyer, P. v. R. In *The Chemistry of Organic Silicon Compounds*; Rappoport, Z., Apeloig, Y., Eds.; John Wiley & Sons, 2001; Vol. 3, pp 1–163, Chapter 1.
- (2) (a) Weidenbruch, M.; Willms, S.; Saak, W.; Henkel, G. *Angew. Chem., Int. Ed.* **1997**, *36*, 2503.
- (3) (a) Ichinohe, M.; Sanuki, K.; Inoue, S.; Sekiguchi, A. *Silicon Chem.* **2005**, *3*, 111. (b) Uchiyama, K.; Nagendran, S.; Ishida, S.; Iwamoto, T.; Kira, M. *J. Am. Chem. Soc.* **2007**, *129*, 10638.
- (4) Trinquier, G.; Malrieu, J.-P. *J. Am. Chem. Soc.* **1981**, *103*, 6313.
- (5) Steinmetz, M. G.; Udayakumar, B. S.; Gordon, M. S. *Organometallics* **1989**, *8*, 530.
- (6) (a) Yoshizawa, K.; Kang, S.-Y.; Yamabe, T.; Naka, A.; Ishikawa, M. *Organometallics* **1999**, *18*, 4637. (b) Yoshizawa, K.; Shiota, Y.; Kang, S.-Y.; Yamabe, T. *Organometallics* **1997**, *16*, 5058.
- (7) Sakai, S. *J. Mol. Struct. (Theochem)* **1999**, *283*, 461–462.
- (8) Müller, T. In *Organosilicon Chemistry IV. From Molecules to Materials*; Auner, N., Weis, J., Eds.; VCH, 2000; pp 110–116.
- (9) Koch, R.; Bruhn, T.; Weidenbruch, M. *J. Mol. Struct. (Theochem)* **2004**, *680*, 91.
- (10) Zhao, M.; Gimarc, B. M. *Inorg. Chem.* **1996**, *35*, 5378.
- (11) Fernández, I.; Frenking, G. *Chem. Eur. J.* **2006**, *12*, 3617.
- (12) Glendening, E. D.; Reed, A. E.; Carpenter, J. E.; Weinhold, F. NBO, Version 3.1.
- (13) Weinhold, F.; Landis, C. R. In *Valency and Bonding. A Natural Bond Orbital Donor-Acceptor Perspective*; Cambridge University Press: New York, 2005; pp 182–191, Chapter 1.
- (14) (a) Mo, Y.; Peyerimhoff, S. D. *J. Chem. Phys.* **1998**, *109*, 1687. (b) Mo, Y.; Song, L.; Lin, Y. *J. Phys. Chem. A* **2007**, *111*, 8291.
- (15) Koch, W.; Holthausen, M. C. *A Chemist's Guide to Density Functional Theory*; Wiley-VCH, 2000.
- (16) Parr, R. G.; Yang, W. *Density-Functional Theory of Atoms and Molecules*; Oxford University Press: New York, 1989.
- (17) Becke, A. D. *J. Chem. Phys.* **1993**, *98*, 5648.
- (18) (a) Lee, C.; Yang, W.; Parr, R. G. *Phys. Rev. B* **1988**, *37*, 785. (b) Vosko, S. H.; Wilk, L.; Nusair, M. *Can. J. Phys.* **1980**, *58*, 1200.
- (19) For first-row elements (a) Krishnan, R.; Binkley, J. S.; Seeger, R.; Pople, J. A. *J. Chem. Phys.* **1980**, *72*, 650. For second-row elements (b) McLean, A. D.; Chandler, G. S. *J. Chem. Phys.* **1980**, *72*, 5639.
- (20) Polarization and diffuse functions in the basis set were found to be important for the geometry optimization of 1,3-butadiene. Xi, H.-W.; Li, W.-Z.; Liu, F.-L.; Huang, M.-B. *J. Mole. Struct. (Theochem)* **2004**, *683*, 71.
- (21) Møller, C.; Plesset, M. S. *Phys. Rev.* **1934**, *46*, 618.
- (22) Pople, J. A.; Binkley, J. S.; Seeger, R. *Int. J. Quantum Chem.* **1976**, *10*, 1.
- (23) Cizek, J. *Adv. Chem. Phys.* **1969**, *14*, 35.
- (24) Purvis, G. D.; Bartlett, R. J. *J. Chem. Phys.* **1982**, *76*, 1910.
- (25) Scuseria, G. E.; Janssen, C. L.; Schaefer, H. F., III. *J. Chem. Phys.* **1988**, *89*, 7382.
- (26) (a) Scuseria, G. E.; Schaefer, H. F., III. *J. Chem. Phys.* **1989**, *90*, 3700. (b) Ragavachari, K.; Trucks, G. W.; Pople, J. A.; Head-Gordon, M. *Chem. Phys. Lett.* **1989**, *157*, 479. (c) Woon, D. E.; Dunning, T. H., Jr. *J. Chem. Phys.* **1993**, *98*, 1358. (d) Dunning, T. H., Jr. *J. Chem. Phys.* **1989**, *90*, 1007.
- (27) Frisch, M. J.; Trucks, G. W.; Schlegel, H. B.; Scuseria, G. E.; Robb, M. A.; Cheeseman, J. R.; Montgomery, J. A., Jr.; Vreven, T.; Kudin, K. N.; Burant, J. C.; Millam, J. M.; Iyengar, S. S.; Tomasi, J.; Barone, V.; Mennucci, B.; Cossi, M.; Scalmani, G.; Rega, N.; Petersson, G. A.; Nakatsuji, H.; Hada, M.; Ehara, M.; Toyota, K.; Fukuda, R.; Hasegawa, J.; Ishida, M.; Nakajima, T.; Honda, Y.; Kitao, O.; Nakai, H.; Klene, M.; Li, X.; Knox, J. E.; Hratchian, H. P.; Cross, J. B.; Bakken, V.; Adamo, C.; Jaramillo, J.; Gomperts, R.; Stratmann, R. E.; Yazyev, O.; Austin, A. J.; Cammi, R.; Pomelli, C.; Ochterski, J. W.; Ayala, P. Y.; Morokuma, K.; Voth, G. A.; Salvador, P.; Dannenberg, J. J.; Zakrzewski, V. G.; Dapprich, S.; Daniels, A. D.; Strain, M. C.; Farkas, O.; Malick, D. K.; Rabuck, A. D.; Raghavachari, K.; Foresman, J. B.; Ortiz, J. V.; Cui, Q.; Baboul, A. G.; Clifford, S.; Cioslowski, J.; Stefanov, B. B.; Liu, G.; Liashenko, A.; Piskorz, P.; Komaromi, I.; Martin, R. L.; Fox, D. J.; Keith, T.; Al-Laham, M. A.; Peng, C. Y.; Nanayakkara, A.; Challacombe, M.; Gill, P. M. W.; Johnson, B.; Chen, W.; Wong, M. W.; Gonzalez, C.; Pople, J. A. *Gaussian 03*, revision B.05; Gaussian, Inc.: Wallingford, CT, 2004.
- (28) (a) Schmidt, M. W.; Baldrige, K. K.; Boatz, J. A.; Elbert, S. T.; Gordon, M. S.; Jensen, J. H.; Koseki, S.; Matsunaga, N.; Nguyen, K. A.; Su, S.; Windus, T. L.; Dupuis, M.; Montgomery, J. A. *J. Comput. Chem.* **1993**, *14*, 1347–1363. (b) B3LYP in GAMESS uses VWN5 functional for local correlation.
- (29) Stereochemical definitions and notations: Moss, G. P., *Appl. Chem.* **1996**, *68*, 2193.
- (30) The PES for internal rotation was conducted on **13** (although it is not a minimum and is slightly higher in energy).
- (31) (a) The significantly larger radial extension of 3p(Si) orbital relative to that of 2p(C) orbital^{13,1b} leads to the following trend in p-orbital overlap (S): 3p(Si)–3p(Si) > 3p(Si)–2p(C) > 2p(C)–2p(C) (at the same bond distances); e.g., the 3p(Si)–3p(Si) atomic orbital overlap (S(AO)) in **6** and the 2p(C)–2p(C) S(AO) in **5** are 0.380 and 0.203, respectively (at B3LYP/STO-3G, constraining the Si–Si bond length in **6** to 1.427 Å, which is the optimized C–C bond length in **5**). However, in optimized **6**, $r(\text{Si}–\text{Si}) = 2.298$ Å, and the 3p(Si)–3p(Si) S(AO) drops significantly to 0.102, leading to a smaller internal rotation barrier in **6** in comparison to **5**. The above mentioned trend in S(AO) is also obtained in the calculated $p(\text{M}^1)–p(\text{M}^2)$ S(AO) in $\text{H}_2\text{M}^1=\text{M}^2\text{H}_2$ (C_{2h} symmetry, at $r(\text{M}^1=\text{M}^2) = 2.14$ Å). Thus, for $\text{M}^1=\text{M}^2=\text{Si}$, $\text{M}^1=\text{Si}$, $\text{M}^2=\text{C}$, and $\text{M}^1=\text{M}^2=\text{C}$, those S(AO) are 0.133, 0.082, and 0.048, respectively. In $\text{H}_2\text{Si}=\text{CH}_2$ or dienes that contain a Si=C bond, the p-orbital overlap is also affected by the polarity of the bond.¹⁸ The conclusion from these data is that the central dienic single bond length is the major factor that controls the internal rotation barrier. The inherent trend of S(AO) at a particular bond distance is actually opposite to the observed trend in the internal rotation barriers, and the conclusion therefore is that it is overridden by other factors. (b) Kutzelnigg, W. *Angew. Chem., Int. Ed. Engl.* **1984**, *23*, 272.
- (32) (a) The optimized double-bond lengths in the s-trans conformers of **3** and **4** calculated at B3LYP in this study are somewhat longer than those calculated at HF/d $\zeta + d(\text{Si})$,⁴ and the central single-bonds are somewhat shorter, e.g., at HF $r(\text{Si}=\text{C})$ and $r(\text{C}–\text{C})$ are 1.705 and 1.445 Å, respectively.⁴ Our B3LYP/6-311+G(d,p) optimized geometry of the s-cis conformer of **5** is almost equal to Yoshizawa's⁶ B3LYP/6-31G(d,p) optimized geometry. On the other hand, the B3LYP/6-311+G(d,p) optimized geometry of gauche **5** is considerably different from that calculated by Sakai at CASSCF/6-31G(d,p).⁷ For example, $r(\text{Si}=\text{C}) = 1.819$ Å at CASSCF/6-31G(d,p), compared to 1.739, 1.735, and 1.734 Å, respectively, at B3LYP, MP2, and CCSD/6-311+G(d,p). The optimized bond lengths of the gauche conformer of 1,3-disilabutadiene (**7**) calculated at CASSCF/6-31G(d,p)⁷ are close to ours, but the SiCCSi dihedral angle of 24.3°⁷ is larger than 11.3° calculated at B3LYP/6-311+G(d,p) but smaller than the values of 37.3 and 36.3° calculated at MP2/6-311+G(d,p) and CCSD/6-311+G(d,p), respectively. (b) The optimized geometries of the s-trans and s-cis conformers of **11** are similar to those calculated at B3LYP/6-31G(d,p).⁹
- (33) March, J. *Advanced Organic Chemistry*, 4th Ed.; Wiley & sons: New York, 1992.
- (34) Structural evidence for π -conjugation in 1,3-butadiene: Craig, N. C.; Groner, P.; McKean, D. C. *J. Phys. Chem. A* **2006**, *110*, 7461.
- (35) $\Delta E(\pi_a \rightarrow \pi_b^*)$ and F_{ab^*} in **6** at $r(\text{Si}–\text{Si})$ constrained to 1.427 Å are 46.8 kcal/mol and 0.089 hartree, respectively (B3LYP/6-311+G(d,p)), significantly larger than the values for **5** at $r(\text{C}–\text{C}) = 1.427$ Å and in marked contrast to the trend calculated by using the longer optimized $r(\text{Si}–\text{Si})$ of 2.298 Å in **6** (Table 4).
- (36) (a) We compare VRE to NBO results because both calculations are done at the geometry of the delocalized ground state. (b) The trend in π -conjugation energies calculated by Energy Decomposition Analysis (EDA) is (kcal/mol) **5** (32.8) > **3** (24.8) > **12** (19.5) > **7** (16.4) > **8** (13.4) > **4** (12.0) > **6** (8.8),¹¹ the same as that calculated by using either

BLW or NBO methods; however, the EDA energies lie in between the VREs and the NBO π -conjugation energies.

(37) Hehre, W. J.; Radom, L.; Schleyer, P. V. R.; Pople, J. A. In *Ab initio Molecular Orbital Theory*; John Wiley & Sons: New York, 1986; pp 298–308, Chapter 6.

(38) Wodrich, M. D.; Wannere, C. S.; Mo, Y.; Jarowski, P. D.; Houk, K. N.; Schleyer, P. V. R. *Chem. Eur. J.* **2007**, *13*, 7731.

(39) Kistiakowsky, G. B.; Ruhoff, J. R.; Smith, H. A.; Vaughan, W. E. *J. Am. Chem. Soc.* **1936**, *58*, 146.

(40) (a) π -Conjugation energy of 8.6 kcal/mol was measured experimentally^{40b} for 1,3-butadiene from the difference between the experimental heat of hydrogenation of 1,3-butadiene of -57.1 kcal/mol³⁹ and that of two molecules of ethylene which lack resonance stabilization ($\Delta H_{\text{exp}} = -65.7$ ³⁹). Taking into account the two protobranching 1–3-interactions of ca. 2.8 kcal/mol each,³⁸ which stabilizes *n*-butane, the hydrogenation product of 1,3-butadiene, leads to a π -conjugation energy of 14.2 kcal/mol. This value is in good agreement with the resonance energy calculated by bond separation energies (BSE) (see also ref 38) and with the VRE (14.4 kcal/mol, Table 6), but it is significantly smaller than that calculated by using the NBO method (27.5 kcal/mol). The π -conjugation energies calculated for 1,3-butadiene by using the energy decomposition analysis (EDA) is 19.5 kcal/mol.¹¹ (b) Mo, Y *J. Chem. Phys.* **2003**, *119*, 1300.

(41) Note that only eq 5 is isodesmic; eqs 4 and 6 are not.

(42) Shaik, S, Hiberty, P. C. *A Chemist's Guide to Valence Bond Theory*; Wiley- InterScience, 2007.

(43) (a) The effect of π -conjugation in structures **8**, **9**, **10**, and **11** is probably slightly overestimated, because, in BLW, we used planar structures. (b) **11** is exceptional because of the large distortion from planarity in the fully optimized *s*-trans (C_2) structure.

(44) Except for the resonance energies calculated by using eq 2, where $R^2 = 0.684$, which also do not follow the trend found in resonance energies calculated by either NBO or BLW.

(45) **11** has been excluded from the correlation. Its rotation barrier is smaller than expected from the calculated π -conjugation energies with all methods of calculation.

(46) Weinhold, F.; Landis, C. R. In *Valency and Bonding: A Natural Bond Orbital Donor-Acceptor Perspective*; Cambridge University Press, 2005; pp 226–252, Chpater 3.4.2.

(47) Similar conclusions were obtained regarding the rotation barrier in allyl cation, allyl anion, and allyl radical in a report by Mo, Y.; Song, L.; Lin, Y. *J. Phys. Chem. A* **2007**, *111*, 8291.

(48) Schreiner, P. R. *Angew. Chem., Int. Ed.* **2002**, *41*, 3579.

(49) Brunk, T. K.; Weinhold, F. *J. Am. Chem. Soc.* **1979**, *101*, 1700.

(50) Goodman, L.; Pophristic, V.; Weinhold, F. *Acc. Chem. Res.* **1999**, *32*, 983.

(51) Weinhold, F. *Nature* **2001**, *411*, 539.

(52) Pophristic, V.; Goodman, L. *Nature* **2001**, *411*, 565.

(53) Mo, Y.; Wu, W.; Song, L.; Lin, M.; Zhang, Q.; Gao, J. *Angew. Chem., Int. Ed.* **2004**, *43*, 1986.

JP803837H